Operational GHG Emissions Assessment – Site C

Operating Year 1 – Annual Assessment

BC Hydro

29 April 2026

→ **The Power of Commitment**

<table>
<tr><th>Project name</th><td colspan="7">BC Hydro Operations GHG Monitoring Site C</td></tr>
<tr><th>Document title</th><td colspan="7">Operational GHG Emissions Assessment – Site C | Operating Year 1 – Annual Assessment</td></tr>
<tr><th>Project number</th><td colspan="7">12671172</td></tr>
<tr><th>File name</th><td colspan="7">12671172-GHD-00-00-EN-RPT-0010.docx</td></tr>
<tr><th rowspan="2">Status Code</th><th rowspan="2">Revision</th><th rowspan="2">Author</th><th colspan="2">Reviewer</th><th colspan="3">Approved for issue</th></tr>
<tr><th>Name</th><th>Signature</th><th>Name</th><th>Signature</th><th>Date</th></tr>
<tr><td>S4</td><td>00</td><td>John Taylor</td><td>Deacon Liddy</td><td>Deacon Liddy</td><td>Deacon Liddy</td><td>Deacon Liddy</td><td>April 29, 2026</td></tr>
</table>

Draft versions of this assessment were reviewed by Dr. Zaher Hashisho (University of Alberta) between February and April 2026. Comments provided by Dr. Hashisho were incorporated to refine the assessment. GHD gratefully acknowledges Dr. Hashisho's contributions.

GHD
Contact: John Taylor | GHD
138 East 7th Avenue, Suite 100
Vancouver, British Columbia V5T 1M6, Canada
T +1 604 214 0510 | **F** +1 604 214 0525 | **E** info-northamerica@ghd.com | **ghd.com**

Executive summary

Introduction and Regulatory Context

GHD Limited (GHD) was retained by the British Columbia Hydro and Power Authority (BC Hydro) to conduct post-impoundment greenhouse gas (GHG) emissions monitoring and reporting for the Site C Clean Energy Project (Site C), located near Fort St. John, British Columbia. This work is undertaken to fulfill the requirements of Condition 65 of Environmental Assessment Certificate #14-02, issued by the British Columbia Environmental Assessment Office (BC EAO). Condition 65 requires the development and implementation of a robust Greenhouse Gases Monitoring and Follow-Up Program to validate the predictions of the GHG model completed during the environmental assessment phase and to quantify net GHG emissions from the Site C reservoir during the first ten years of operation.

This report presents the Operational GHG Emissions Assessment (Operational Assessment) for Operating Year 1, summarizing monitoring activities and emissions estimates for the period from April 1, 2025, to March 31, 2026.

Objectives and Scope

The primary objectives of this Operational Assessment are to:

- Quantify GHG emissions from the Site C reservoir during the first year of operation using direct measurement-based methods.
- Characterize spatial and temporal variability in emissions across the reservoir domain.
- Compare observed operational emissions with baseline (pre-impoundment) conditions and modelled predictions prepared during the environmental assessment.

The assessment focuses on the primary GHG emission pathways associated with hydroelectric reservoirs, including reservoir surface emissions (diffusion and ebullition), degassing emissions, and downstream diffusive emissions evaluated through comparison to baseline conditions.

Monitoring Program and Methodology

Operational GHG emissions were quantified using an integrated monitoring approach designed to balance spatial coverage and temporal resolution across the large and heterogeneous Site C reservoir domain. The monitoring program was implemented in accordance with the approved Operational Phase Monitoring Plan and incorporated the following methods:

- Eddy Covariance (EC) Systems – Two eddy covariance systems were deployed along the reservoir perimeter to continuously measure net fluxes of carbon dioxide (CO_2) and methane (CH_4). One system was located near the dam to capture emissions from the lower reservoir, including areas influenced by spillways and turbines, while the second system was installed near the Bear Flat area to represent mid-reservoir conditions and potential emission hotspots associated with pre-impoundment wetlands. EC data provide high-frequency, near-continuous measurements and were used primarily to characterize diurnal and seasonal variability in emissions.
- Flux Chamber Monitoring – Static floating flux chambers were deployed monthly at multiple locations across defined reservoir segments to capture spatial variability in diffusive GHG emissions, particularly in shallow and near-shore areas not fully represented by the EC footprints. Flux chamber measurements were conducted during ice-free periods and were integrated with EC-derived temporal patterns to extrapolate emissions across the full reservoir area and reporting period.
- Dissolved Carbon Measurements – Degassing emissions were estimated using dissolved inorganic carbon (DIC) concentrations measured upstream and downstream of the dam, combined with water discharge data. Differences in DIC concentrations were conservatively attributed to CO_2 emissions associated with turbine and spillway passage.

These complementary datasets were integrated to estimate monthly and cumulative reservoir GHG emissions for the reporting period.

Results and Key Findings

- Temporal Variability – Eddy covariance measurements showed clear diurnal variability in CO_2 flux, with higher emissions typically observed during nighttime hours and lower emissions during daytime periods. Methane flux exhibited less consistent diurnal behaviour, reflecting the episodic and spatially heterogeneous nature of CH_4 production and release in reservoir systems.

  Seasonally, both CO_2 and CH_4 fluxes were generally higher during warmer months, with peak emissions observed in summer and early autumn. Reduced emissions were observed during late autumn and early winter, although data availability during colder periods was limited by extreme weather conditions and equipment downtime.
- Spatial Variability – Flux chamber measurements demonstrated substantial spatial variability in emissions across reservoir segments. In general, CO_2 flux tended to decrease with increasing distance upstream from the dam, while CH_4 flux did not exhibit a consistent spatial trend. Elevated CH_4 emissions were observed in segments associated with pre-impoundment wetlands and river deltas, particularly near the Halfway River confluence, indicating the influence of organic-rich substrates.

  Segments located approximately 50 km downstream of the dam (Segment A) were monitored for comparison with baseline conditions. Fluxes measured at this location were generally within, or near the upper end of, baseline ranges for the Peace River. Comparisons between downstream segments immediately below the dam and those farther downstream did not support clear attribution of downstream diffusive emissions to dam-related processes during the reporting period.
- Degassing Emissions – Degassing emissions estimated from dissolved carbon measurements contributed a measurable portion of total CO_2 emissions. Monthly degassing estimates varied in response to changes in water throughput, while variability in individual DIC measurements necessitated the use of averaged concentration differences to provide a conservative and stable estimate.
- Cumulative and Net Emissions – For the monitoring period, total cumulative reservoir GHG emissions were quantified by integrating spatially distributed flux chamber data, temporally resolved EC measurements, and degassing emissions. When compared with pre-impoundment baseline emissions estimated in the Baseline GHG Emissions Assessment, operational emissions during the monitoring period were substantially higher, reflecting the influence of reservoir creation and early operational conditions.

  Using the operational emissions and the established baseline, net GHG emissions for Operating Year 1 were calculated. These results indicate that first-year operational emissions exceed baseline conditions and lower-tier model estimates, while being less than Tier 3 model predictions.

Limitations

The Operational Assessment is subject to, and must be read in conjunction with, the limitations set out in Section 4.4 and the assumptions and qualifications contained throughout the Operational Assessment.

Contents

Table index

Figure index

Appendices

1. Background

GHD Limited (GHD) was retained by the British Columbia Hydro and Power Authority (BC Hydro) to perform post-impoundment greenhouse gas (GHG) emissions monitoring and reporting for the Site C Clean Energy Project (Site C) near Fort St. John, British Columbia (BC). The monitoring component is ongoing, while the reporting component is this Operational GHG Emissions Assessment (Operational Assessment).

The objective of the Operational Assessment is to support BC Hydro's commitment to GHG emissions monitoring for Site C, as required by Condition 65 of Environmental Assessment Certificate (EAC) #14-02, issued by the British Columbia Environmental Assessment Office (BC EAO). Condition 65 mandates the development of a robust and defensible Greenhouse Gases Monitoring and Follow-Up Program (the Monitoring Program) to validate the predictions of the GHG model completed as part of the environmental assessment application (prepared by Stantec Consulting Ltd., December 2012). Condition 65 specifies that the Monitoring Program must include protocols for monitoring and reporting GHG emissions from the Site C reservoir for the first 10-years of operation, including emissions from both operation and maintenance activities.

In support of meeting these requirements, GHD previously developed the Operational Phase Monitoring Plan (Monitoring Plan), which outlined the monitoring and reporting activities to be undertaken during Site C operations to monitor and estimate net emissions from the entire reservoir domain with reasonable accuracy.

GHD has since prepared this Operational Assessment per the activities described in the Monitoring Plan. The purpose of the Operational Assessment is to describe and present the monitoring activities and emissions quantification undertaken from April 1, 2025, to March 31, 2026 (Reporting Period). Per EAC #14-02, the Reporting Period was to begin within 180-days of the commencement of facility operations.

As further described in the Monitoring Plan, net emissions are defined as the changes in emissions within the reservoir footprint caused by the creation of the reservoir, accounting for exchanges occurring before, during, and after project construction. It is important to note the numerous variables involved in emissions conditions within Site C's large domain. There make it essential to integrate multiple methods to develop a comprehensive estimation approach for the entire domain.

In general, studies of GHG emissions from freshwater reservoirs have recently evolved to better understand the emissions from hydroelectric facilities, serving as renewable and low-carbon electricity sources, in comparison to conventional fossil fuel plants. Net emissions from reservoirs can vary depending on ecosystem types and components within the reservoir footprint area before impoundment. Prior to the Operational Assessment and Monitoring Plan, GHD completed the Baseline GHG Emissions Assessment (Baseline Assessment). The results of the Operational Assessment and Baseline Assessment will be used in tandem to determine net emissions.

The following sections provide the relevant background information, monitoring activities, quantification methodologies, and results for the first year of operational GHG emissions monitoring.

1.1 Assessment Scope

The scope of the Operational Assessment encompasses the monitoring and reporting of GHG emissions from the Site C reservoir during the initial year of operation. It includes detailed descriptions of the specific monitoring and calculation methods used and presents the quantified annual emissions. Additionally, the Assessment compares the operational emissions to both the baseline and modelled emissions, the former of which provides a measurement of net GHG emissions resulting from the impoundment of the Site C reservoir.

1.2 Site C Reservoir Area Understanding

Site C Clean Energy Project is located in Fort St. John, BC. Site C reservoir area extends west of Fort St. John up the Peace River. The maximum normal operating range for the Site C reservoir is 1.8 m — between 460.0 m and 461.8 m.

However, during typical operations the reservoir is expected to fluctuate within a smaller range. The Site C reservoir is approximately 83 km long and, on average, two to three times the width of the pre-impoundment river. The reservoir flooded approximately 6,357 hectares (ha) of land, resulting in a total surface area, including the pre-impoundment river area, of approximately 9,330 ha. The 461.8 m elevation boundary is used to quantify the post-impoundment reservoir footprint area.

Figure 1.1 shows the site location map including the reservoir area.

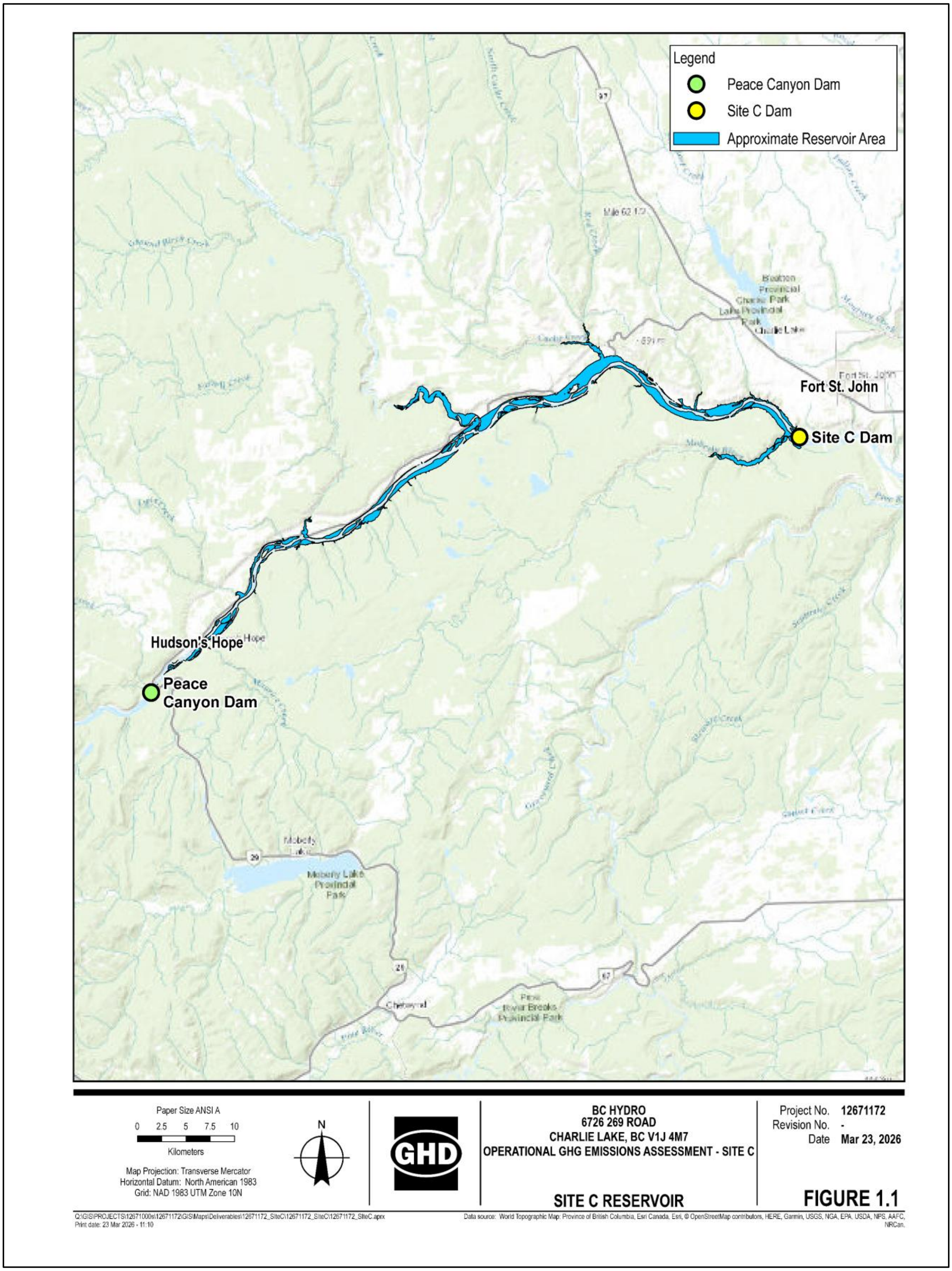

Figure 1.1 ***Estimated reservoir extent***

2. Emission Pathways from Reservoirs

The GHG emission pathways in boreal hydroelectric reservoirs include diffusion at the reservoir surface, bubbling, and downstream emissions, which consist of degassing at the turbines and downstream diffusive emissions (Demarty and Tremblay, 2017). Plant stems on the benthic surface are understood to be a negligible emission source in boreal waters. Of the non-negligible sources, degassing and downstream diffusive emissions are only expected after impoundment of the reservoir area, while other pathways may be present both pre- and post-impoundment. The following sections provide more information for each pathway of the following pathways:

- Diffusive – Reservoir
- Ebullition – Reservoir
- Degassing – Downstream
- Diffusive – Downstream

2.1 Diffusive Emissions – Reservoir

Diffusive emissions occur when gas concentrations in the water become greater than in the atmosphere. The dissolved gases travel across the water-air interface and are emitted to the atmosphere. Flooding of carbon-rich soils causes production of diffusive CO_2 emissions (Jager et al., 2022). CO_2 diffusive emissions are increased in areas with greater temperatures or organic material and are usually observed in deep areas of reservoirs (Jager et al., 2022). Higher CH_4 diffusion rates are usually observed if there is a large amount of organic material with favouring methanogenesis conditions and it is more significant in high surface area reservoirs.

Diffusive emissions can be a challenge to estimate, as they typically have high spatial and temporal variance within a reservoir (Rust et al., 2022). For the Operational Assessment, diffusive emissions were measured using static floating chambers and eddy covariance (EC) systems.

2.2 Emissions from Ebullition – Reservoir

Compared to CO_2 and N_2O, CH_4 is less soluble in water and will form bubbles when produced in water (Deemer et al., 2016). CH_4 ebullition emissions occur in shallow areas of reservoir where the hydrostatic pressure is insufficient to dissolve the gas in the water (IHA/UNESCO, 2010). Also, they can be expected in areas with enough depth that bubbles can form, but not too deep that oxidation occurs before the bubbles reach the water surface, usually in areas 3 – 6 m deep (Jager et al., 2022). The CH_4 ebullition emissions may increase during drawdowns or high temperatures at the shallower areas of the reservoir with abundant vegetation and depending on the conditions, the ebullition fluxes may vary from 0 to 99.6% of the total CH_4 flux from reservoir water surfaces (Deemer et al., 2016) with a global average contribution of 65% of the total CH_4 emissions from freshwaters (Jager et al., 2022). Demarty and Tremblay (2017) found that bubbling contributed much less to overall emissions than diffusive fluxes in Canada.

For the Operational Assessment, while GHD observed the release of discrete bubbles from submerged sediment, it was determined that a quantification of emissions from ebullition specifically was not required. Instead, ebullition was implicitly quantified alongside diffusive emissions using EC systems. While direct measurement of emissions from ebullition specifically has previously been done using inverted funnels and acoustic techniques (Deemer et al., 2016), neither method was determined to be suitable for quantifying the observed ebullition occurring in shallow waters (depth < 0.5 m).

2.3 Degassing Emissions – Downstream

Degassing emissions occur when water drawn from the reservoir passes through the turbines and spillway in the generating station. The sudden pressure-drop and aeration cause the dissolved gases to be emitted. The monitoring area for this type of emissions would include all downstream areas with emissions that are higher than background/baseline. Higher degassing emissions would be expected if water is drawn from the deeper part of the reservoir due to the higher pressure and GHG concentrations compared to water at the surface (Deemer et al., 2016). The proportion of total emissions that come from degassing varies from 1% to 90%, depending on the design of the dam and the GHG concentrations within the reservoir (UNESCO/IHA, 2010).

Degassing emissions can be estimated by determining the difference in the gas concentration upstream and downstream of the dam by taking water samples and multiplying the concentrations by the discharge flow rate (UNESCO/IHA, 2010).

2.4 Diffusive Emissions – Downstream

The influence of degassing emissions can be observed from up to 50 km downstream of dams (Demarty and Tremblay, 2017). Dissolved CO_2 and CH_4 as well as dissolved and particulate organic carbon pass through the dam and discharges into the downstream water body (IHA/UNESCO, 2010). Downstream diffusive emissions consist of the GHGs produced in the reservoir that are emitted from downstream of the dam via diffusion from the river (Deemer et al., 2016).

Downstream diffusive emissions were quantified close to the dam (within 5 km of the turbine outlets). Flux chamber sampling was used to compare emissions 50 km downstream of the dam to the Baseline Assessment. Intermediate downstream diffusive emissions, occurring from 5 km downstream to 50 km downstream, have not been quantified. Downstream tributaries, land use, and seasonal variations make accurately delineating downstream emissions challenging.

3. Methodology

The completed monitoring activities incorporated a combination of different methodologies, which were integrated to estimate the total emissions from the reservoir with reasonable accuracy. This approach accounted for spatial and temporal variations in emissions as well as all primary emission pathways within the domain. The following sections provide detailed descriptions of each method, including the locations and frequencies of monitoring and sampling efforts.

3.1 Eddy Covariance

EC systems were selected as the monitoring method to obtain near real-time, high-frequency data over the area of the reservoir located within their footprints (approximately 100 times the height of the sensors from the water surface, depending on the exact atmospheric conditions). This method is the only established technique for continuous direct flux emissions measurement over area sources. Using this capability aids in understanding the temporal variation of emissions near the primary emission areas within the domain, facilitating more accurate data extrapolation and total net emissions estimation.

3.1.1 Overview

In order to quantify the GHG emissions from reservoir diffusion and ebullition, two EC systems were positioned on the perimeter of the reservoir, as detailed below:

1. Dam EC System (Site C EC System) - the first system is located in direct proximity to the dam, with a footprint capturing emissions in the area immediately upstream of the dam, spillways, and turbines. The system is located to target the least stable area of the reservoir where higher emissions are expected. The ground is slightly lower than the height of the dam and is higher than the height of the reservoir, with a rock embankment separating the reservoir and the system. The area adjacent to the system is clear of vegetation and buildings, other than the dam.

2. Midstream EC System (Bear Flat EC System) - the second system is located further upstream, on the north bank of the reservoir near the Bear Flat area. This location is intended to be a more representative of the midstream emissions and is in proximity to potential midstream hotspots (i.e. areas of pre-impoundment wetlands). The ground is higher than the height of the reservoir and gradually descends towards the reservoir. The area adjacent to the system is vegetated with grasses and is clear of buildings.

Figure 3.1 and Figure 3.2 show the location of the Site C EC system, while Figure 3.3 and Figure 3.4 show the location of the Bear Flat EC system. The locations were chosen based on anticipated GHG hotspots, prevailing wind directions, terrain, vegetation, and site access.

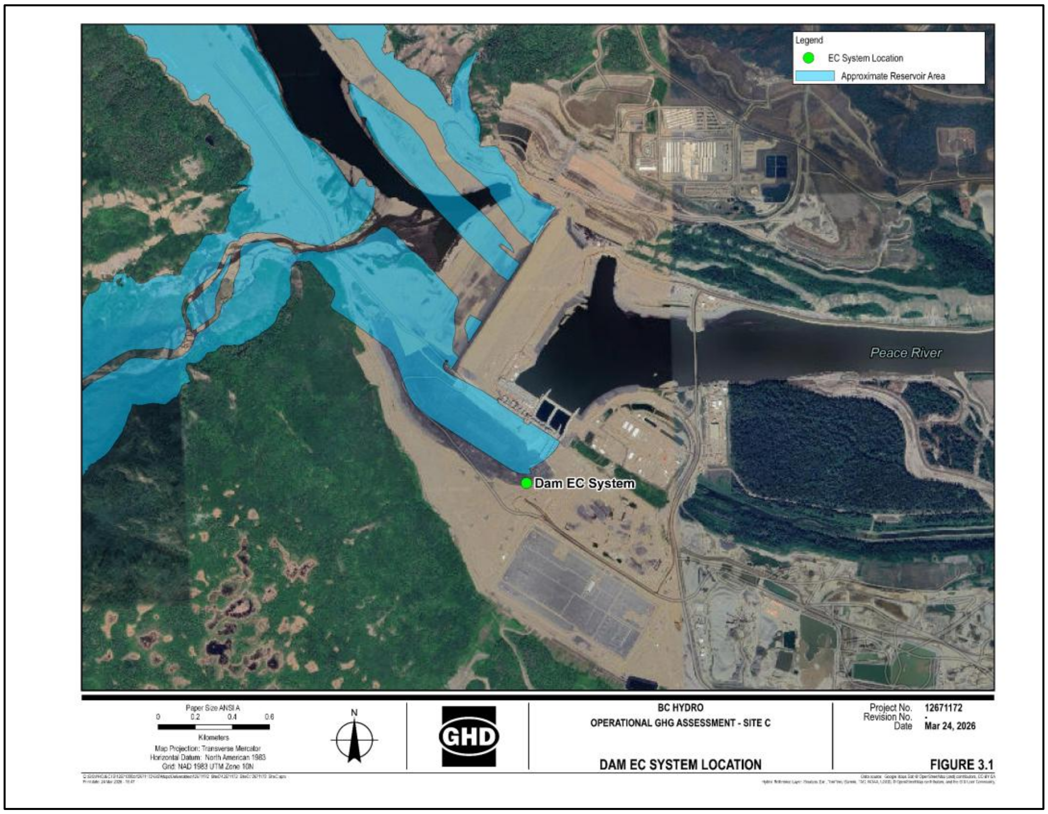

Figure 3.1 *Dam EC System location*

Figure 3.2 *Dam EC System photograph*

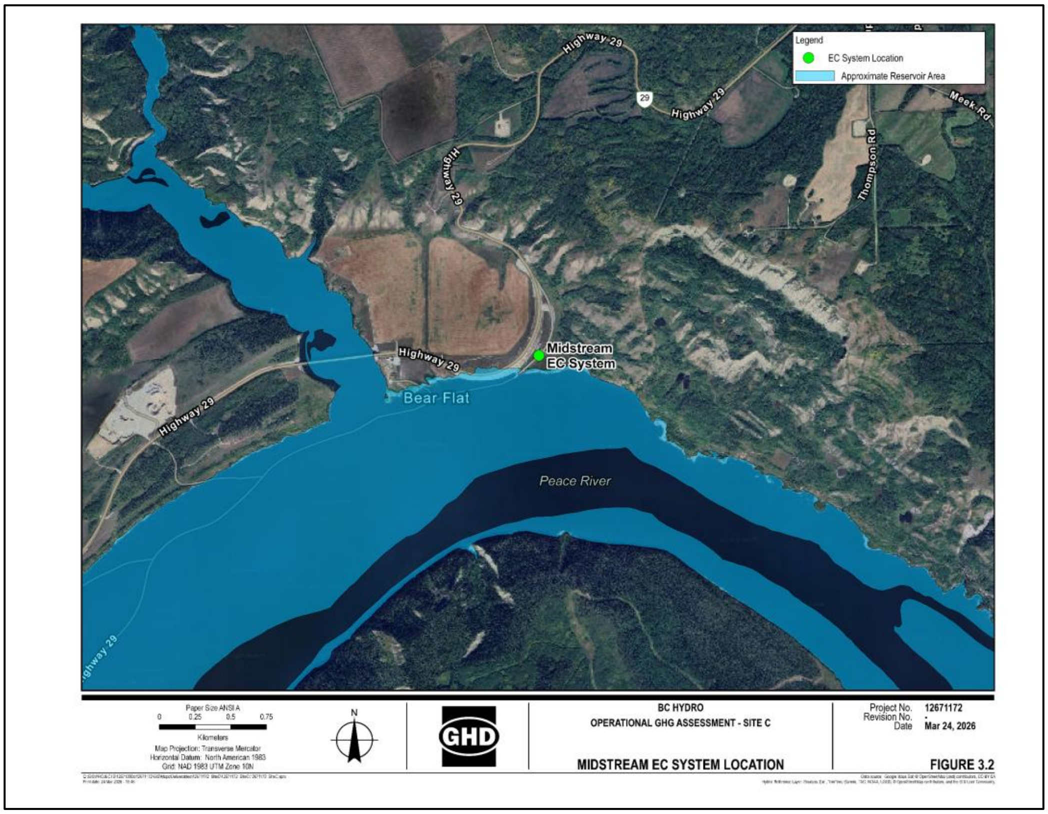

Figure 3.3 Midstream EC System location (near Bear Flat area)

Figure 3.4 Midstream EC System photograph (near Bear Flat area on decommissioned road)

Table 3.1 presents the primary system components and specifications for both EC systems (LI-COR Environmental, 2024) (Gill Instruments, 2024).

Table 3.1 Eddy Covariance System Main Components

Component	Instrument	Specifications
CO_2 Analyzer	LI-7500DS	- CO_2: 0 to 3,000 µmol/mol, ±1% accuracy - H_2O: 0 to 60 µmol/mol, ±1% accuracy - Air Temp: -40 to 70°C, ±0.25°C (-20 to 70°C) - Air Pressure: 20–110 kPa, ±0.4 kPa (50 to 110 kPa)
CH_4 Analyzer	LI-7700	- CH_4: 0–25 ppm @ -25°C, 0–40 ppm @ 25°C, ±1% accuracy
Sonic Anemometer	Gill WindMaster Pro	- Wind Speed: 0 to 65 m/s, 0.01 m/s resolution, <1.5% RMS accuracy @ 12 m/s
Biomet Instruments	Vaisala HMP155	- Humidity and Temperature Probe (0 to 100% RH and -80 to 60ºC)
	Kipp & Zonen NR Lite2	- Net Radiometer (-200 to 1000 W/m^2)
Datalogging and processing	SmartFlux 3 System	- Provides GPS position and time synchronization, connections for digital sonic anemometer data, a USB port for logging data to a USB storage device, and a microcomputer that runs EddyPro Software.
	Data Acquisition Module (DAqM) and Data Retention Module (DRM)	- Data pass-through devices from Biomet instrument to SmartFlux System
Remote control and data Access	- Brainboxes SW-508 network switch - AirLink RV50X Modem SIERRA WIRELESS	- Instrument settings control and data access using cellular communication
Measurement Frequency	All instruments	- Operate at 10 Hz - Data averaged in 1-minute increments - Analyzed in 30-minute batches by EddyPro - Average to hourly for emissions calculations and reporting

Installation of instrumentation on each EC system was done with consideration given to instrument position relative to the reservoir. The CO_2 and CH_4 analyzers were placed on opposite sides of the sonic anemometer. The anemometer and gas analyzers were rotated such that the structural spars of each instrument would have minimal interference with prevailing winds from the reservoir. Additionally, the horizontal member on which the instruments were mounted was placed such that the gas analyzers would not interfere with anemometer readings during periods of winds from the reservoir.

Table 3.2 presents relevant physical parameters of the EC systems.

Table 3.2 Selected EC System Physical Parameters

Parameter	Site C EC Station	Bear Flat EC Station
Latitude, longitude (decimal degrees)	56.18606, -120.9126	56.27525, -121.2152
Anemometer height above ground (m)	9.88	10.69
Anemometer north spar offset (degrees from magnetic north)	37	150
Approximate ground height above reservoir surface (m)	5	10
Approximate horizontal distance from EC system to reservoir (m)	50	105

3.1.2 Outputs

The data from each EC system was analyzed to produce the following outputs:

– Diurnal Emissions Variation – Monthly average fluxes for CO_2 and CH_4 were calculated using corrected and filtered data. For each EC station, flux data from time periods where the predominant wind direction did not originate from the reservoir or spillways were excluded from emissions calculations. Fetch, defined as the upwind distance across a relatively homogenous surface, equivalent to upwind distance over the reservoir surface, was considered for each measurement.

  - At the Site C station, only fluxes recorded during wind directions between 297° and 50° were considered valid. Distance from the instrument to the far source boundary varied depending on exact angle, ranging from approximately 1,150 m to 5,000 m.
  - At the Bear Flat station, only fluxes recorded during wind directions between 110° and 240°, were considered valid. Distance from the instrument to the far source boundary varied depending on exact angle, ranging from approximately 1,200 m to 7,000 m.

– Day/Night Emissions Variation – Average fluxes were computed separately for daytime and nighttime periods, defined on a monthly basis. Periods ranged from 7-hours of daytime and 17-hours of nighttime (December) to 18-hours of daytime and 6-hours of nighttime (June).

– Footprint Analysis – A footprint analysis was conducted to evaluate the contribution of surrounding areas to the measured fluxes and confirm that the data are representative of the reservoir. The flux footprint diagrams include green circles to indicate the locations of x_{90} for each 30-minute period with a calculable footprint included in the analysis. The x_{90} is defined as the distance from the EC station within which 90% of observed emissions originate.

  - At the Site C station, the greatest x_{90} recorded was 1,140 m. The EC footprint was confirmed to fall reasonably within the boundary of the source area for all data points.
  - At the Bear Flat station, the greatest x_{90} recorded was 1,588 m. The EC footprint was confirmed to fall reasonably within the boundary of the source area for all data points.

  For a minority of 30-minute periods, x_{90} was located outside the source area, with a straight line between x_{90} and the EC system crossing the source area. This was determined to be reasonable as x_{90} indicates the point relative to the EC system at which 90% of observed emissions originate between. These emissions do not specifically originate at x_{90} itself.

– Wind Rose Plots – Wind rose plots were developed using the data from EC systems' 3-D anemometers, illustrating the predominant wind directions during the Reporting Period, which inform the footprint filtering and help assess data representativeness.

Data availability varied throughout the Reporting Period. Instrument and system issues resulted in a minority of months having less than two weeks of data from one of the EC systems. Since EC data is primarily used to apply diurnal temporal variation to the flux chamber data, using incomplete months of data was determined to be acceptable. Additionally, for January and February, both EC systems were mostly not operational, with March EC data applied to each month's calculations. Beyond the diurnal temporal variations, seasonal temporal variations were captured by both EC data and flux chamber data, while spatial variations were captured by flux chamber data.

The results of the above are included in the Results section of the Operational Assessment.

3.2 Flux Chambers

Flux chambers were deployed to capture spatial variations in GHG emissions, specifically over the reservoir's shallow areas. The combined results from flux chamber and EC monitoring integrate both spatial and temporal variations, enabling the extrapolation of emissions across the entire reservoir area. Additionally, flux chamber measurements will help identify significant changes in emission hotspot locations during the monitoring program, guiding any necessary relocation of the EC systems.

3.2.1 Overview

To quantify diffusive GHG emissions, flux chamber measurements were conducted once per location per month, during ice-free periods (typically April through November), and when the locations could be accessed safely. To ensure good spatial distribution and consistency for fair monthly comparisons, the reservoir is divided into the following segments:

1. Upstream segments: Defined as 5 km intervals for the first 20 km and 10 km intervals for the remaining reservoir length.
2. Downstream segments: Two 5 km segments, one immediately downstream of the spillways and another 50 km downstream of the dam.

Figure 3.5 and Figure 3.6 show the segment locations. Exact measurement points within each segment were determined based on accessibility and water conditions during each month.

For the months of December through March, ice cover on the reservoir and snow build up along access roads made most sampling points inaccessible. For December, during the sampling conducted mid-month, only the downstream and farthest upstream locations could have flux chamber measurements conducted. For January and February, no flux chamber measurements were conducted. For March, only the downstream and two farthest upstream locations could have flux chamber measurements conducted, with the lack of open water near the shore being a limiting factor. For segments without measurements conducted but with open water for part or all of a given month, measured fluxes from March applied to January and February. As outlined in the monitoring plan, GHG emissions from ice-covered segments of the reservoir are considered negligible, consistent with findings from previous reservoir-emissions studies (UNESCO/IHA, 2010, Teodoru et al., 2012, Demarty and Tremblay, 2017, Prairie et al., 2018). Satellite imagery and field observations were used to estimate the extent of ice cover.

Data from both EC systems and flux chambers were integrated to calculate total reservoir emissions. EC data captures the full temporal range, while flux chamber data ensures comprehensive spatial coverage.

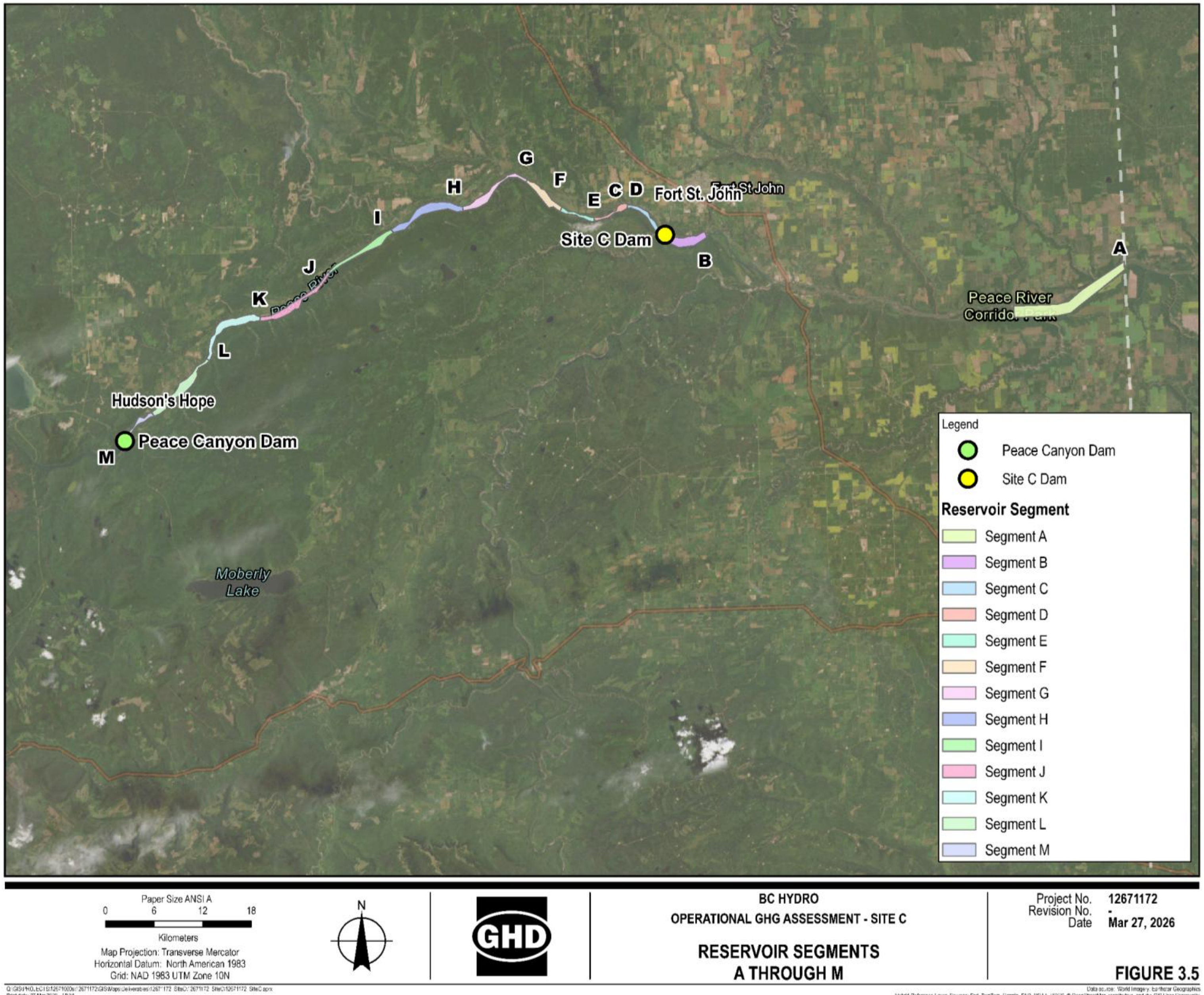

Figure 3.5 Reservoir segments A through M

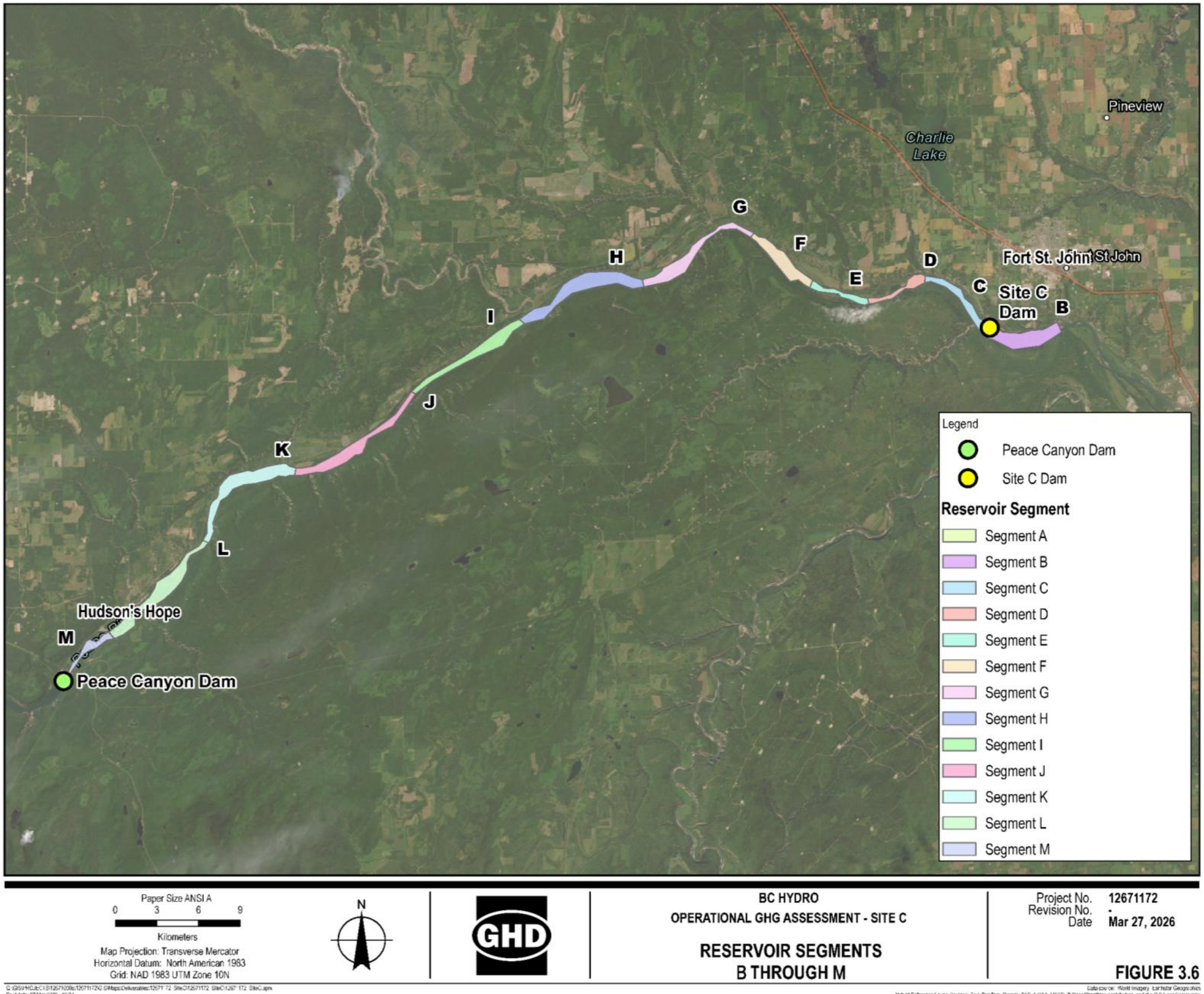

Figure 3.6 Reservoir segments B through M

3.2.2 Flux Chamber Design and System Components

The flux chamber design is a stainless-steel isolation chamber based on the United States Environmental Protection Agency (USEPA) specifications, with a surface area of approximately 0.073 m^2 and a volume of approximately 0.020 m^3. To accommodate measurements on the reservoir surface, a floating system was designed and deployed to minimize interference with the reservoir's natural flow.

The chamber operates in static mode, connected to a $CO_2/H_2O/CH_4$ gas analyzer (LI-7810, LI-COR Biosciences) to continuously measure gas concentrations in a closed-loop system, where the analyzer's outlet directs gases back to the chamber. Two small openings in the top of the chamber allow for the insertion of a thermometer and gas exchange with the atmosphere, which limits pressure build-up.

Readings were recorded at a frequency of 1 Hz over 30-minute measurement periods, with the sum of changes in gas concentrations used to calculate GHG fluxes at each measurement location. Specifically, the sum of all positive changes in concentration of a given gas (x) between measurements was determined. This sum was used with the average pressure (P) during the measurement period, the average temperature (T) during the measurement period, the exact duration (t) of the measurement period, the volume (V) of the flux chamber, the surface area (a) of the flux chamber opening, the universal gas constant (R), and the molar mass (MW) of a given gas (x, CO_2 or CH_4) to determine gas mass flux (j). The equation for the calculation is as follows:

$$j_x = \sum \Delta[x] \cdot \frac{\bar{P} \cdot V}{R \cdot T} \cdot \frac{MW_x}{a} \cdot t$$

As the sum of changes in gas concentration over the entire measurement period were used to determine flux, it is possible that the increase in GHG concentrations in the flux chamber reduced the air-water concentration gradient, thereby decreasing the rate of diffusive emissions. During flux chamber measurements, gas concentrations first increase linearly, then begin to taper as the concentrations of dissolved gases in the water and in the chamber approach an equilibrium. This taper occurs afterer a shorter measurement period over waters with lower dissolved-gas supersaturation, where equilibrium between the chamber and water is reached more quickly. The inclusion of the nonlinear portion of the concentration increases in the data analysis can result in lower calculated emission rates.

Flux chamber data was manually reviewed to identify and remove spikes. Spikes presented as sudden increases and decreases in concentration that exceeded normal changes by an order of magnitude. To be determined to be a spike, concentrations would need to be shown to first increase sharply then decrease to near pre-spike levels. Flux measurements with discrete spikes had spikes removed, while flux measurements with many spikes or a large amount of noise were excluded from emissions calculations.

During summer months, some flux chamber measurements captured ebullition emissions. Field personnel observed discrete bubbles rising through the water, which corresponded with greatly elevated CH_4 concentrations in the flux chamber. In these cases, additional flux chamber measurements were taken in the same segments to measure the flux without ebullition. The averages of these multiple measurements were then used for emissions calculations. Including ebullition emissions in the average is considered conservative and results in some flux outliers, as shown in Section 4.2.

Figure 3.7 and Figure 3.8 depict the flux chamber during sampling.

Figure 3.7 Photograph of flux chamber and gas analyzing during sampling

Figure 3.8 Photograph of flux chamber during sampling

3.3 Dissolved Carbon Measurements

Measurements of dissolved carbon concentrations were chosen as a monitoring method to conservatively quantify degassing emissions. Dissolved carbon was measured in a laboratory following collection and transport of water samples.

3.3.1 Overview

Emissions from turbines and spillways were quantified using dissolved inorganic carbon concentrations of water samples nearby the dam. Samples are taken by Ecofish Research Ltd. or their subconsultants at a variety of locations upstream and downstream of Site C. The locations of water sample points are shown in Figure 3.9.

For the purposes of emissions calculations, dissolved inorganic carbon content immediately upstream of the dam was approximated to the carbon content of the PR3 sample point (~2.1 km upstream of the dam). Dissolved inorganic carbon content (DIC) immediately downstream of the dam was approximated to the carbon content of the PD1 sample point (~13 km downstream of the dam). The difference between the upstream and downstream concentrations was conservatively assumed to be entirely the result of emissions from turbulent water exiting the turbines and flowing over the spillways.

The greater of Peace River discharge rates from the 07FA004 hydrometric station, managed by the Water Survey of Canada (~6 km downstream of the dam) and BC Hydro-provided turbine throughput rates were used with the difference in dissolved inorganic carbon concentrations described above to determine the mass of carbon assumed to be released to atmosphere. All carbon was assumed to be released in the form of CO_2. The mass of carbon was therefore converted to mass of CO_2 and added to the emissions calculated using EC and flux chamber data.

Due to significant monthly variation in DIC, including anomalous results where DIC appeared to increase across the dam, an average of the differences in DIC was used for all monthly degassing emissions calculations.

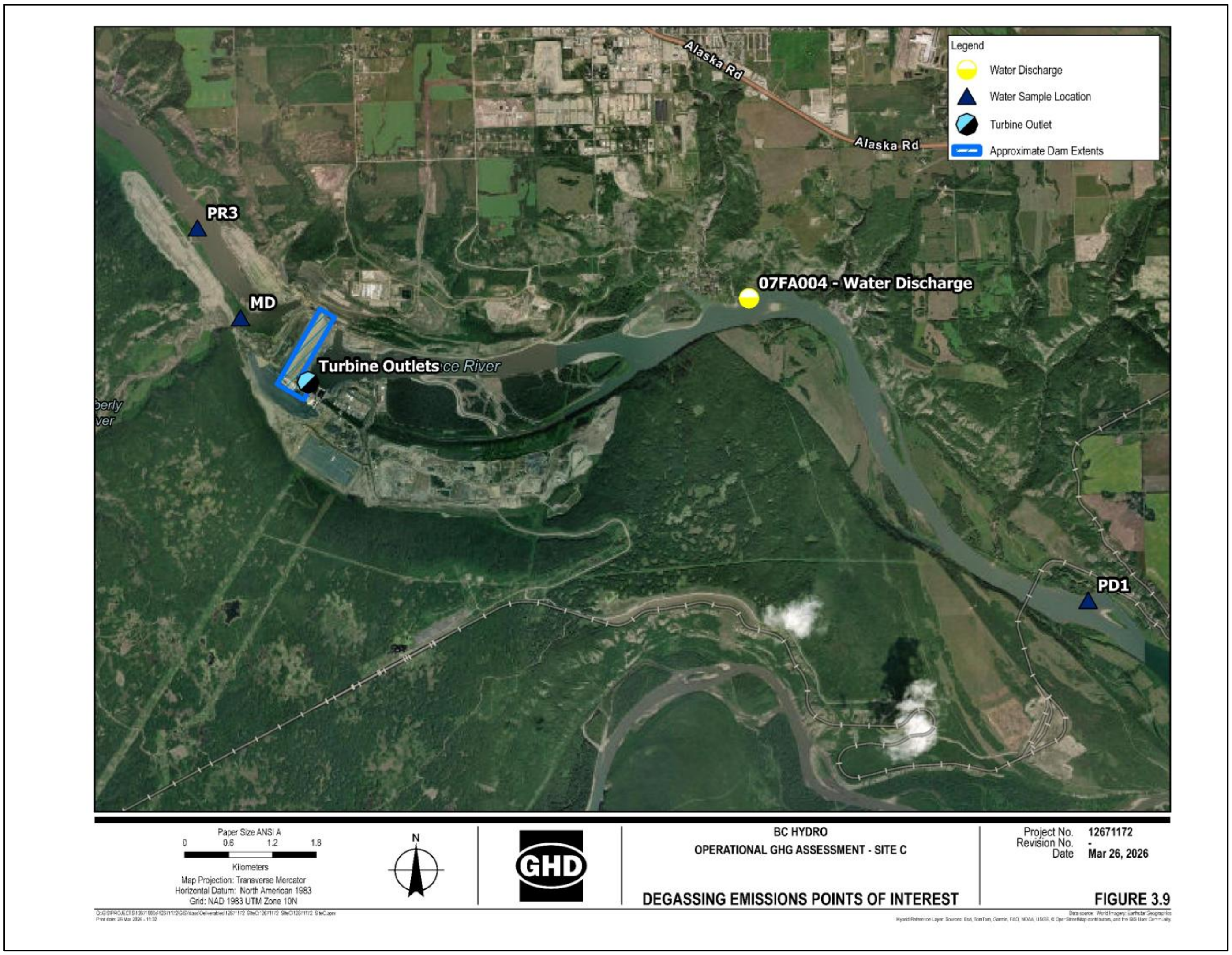

Figure 3.9 Dissolved carbon analysis points of interest

3.3.2 Water Sampling Procedures

Water sampling and analysis were completed by third-parties, with DIC results then used for emissions calculations. Regarding sampling, the following description of procedures has been provided:

"Surface water quality sampling consists of collecting measurements in the field using in situ water quality meters, and collection of water quality samples for laboratory analysis. In situ and laboratory sampling procedures, chain of custody procedures, and quality assurance/quality control (QA/QC) procedures adhered to the guidelines of the British Columbia Field Sampling Manual (Gov BC 2013). Typically, triplicate readings were collected for in situ data, and a field blank and travel blank were collected during each sampling event. In situ measurements and laboratory samples were collected 30 cm below the surface of the water to avoid contamination from any floating surface particulate matter. In situ data were collected with a YSI ProDSS multiparameter digital water quality meter.

Physical parameters, nutrients, anions, bacteriological parameters, total metals, and dissolved metals were measured in the samples collected from surface water quality sites. Laboratory samples were collected in sterile bottles provided by ALS Environmental (ALS); ALS provided preservatives where applicable. Preservation and filtering of laboratory samples followed the British Columbia Field Sampling Manual (Gov BC 2013) and instruction from ALS. A peristaltic pump and silicon tubing were used to fill the sample bottles, and for parameters that require filtration, a Gelman GWV high-capacity groundwater 0.45 µm filter was installed on the outlet tube. A new filter was used at each sample site.

Upon arrival at a sample site, the tubing used with the peristaltic pump and the filter used at that site were flushed with river water for 5 minutes prior to sample collection; the flushing serves to clear any residual carbon from the filters prior to sample collection. The tubing was also flushed with 2 L of deionized water at the end of every sampling day. In most cases, sites were accessible by boat and samples were collected upstream of any effects related to the boat/boat motor, in the main flow in the watercourse away from any back eddy effects or floating debris. Occasionally, flow was considered too low for boat access, at which point field staff collected samples with a telescopic sampling pole from the shore; care was taken to collect samples from representative flowing water conditions. Samples were stored in coolers with ice packs and delivered to the ALS depot in Fort St. John following standard chain of custody procedures. Samples were then shipped either to ALS in either Calgary or Vancouver for analysis."

Additionally, the following information on the analysis of DIC specifically was provided:

"Dissolved Inorganic Carbon is determined on a sample which is filtered through a 0.45 micron filter prior to analysis by the high temperature combustion method with measurement by an infrared detector, where the sample is acidified in a reaction chamber to convert all inorganic carbons (carbonates) to carbon dioxide for analysis."

The use of third-party data was determined to be acceptable for degassing emissions calculations.

3.4 Data Analysis

The following data analysis activities were performed:

1. EC System Measurements – The EC system data analysis was primarily conducted using EddyPro 7.0.9 (LI-COR Biosciences) in Express Mode, with default processing settings. During the data analysis, a combination of the following correction methods was applied:
   - Natural wind coordinate rotation: Rotation of sonic anemometer coordinates to reflect a mean vertical wind speed of zero. The correction was done each 30-minute averaging period.
   - Magnetic declination: Adjustment of wind direction to account for difference between magnetic and geographic north.
   - Time delay compensation: Temporal synchronization of instrument signals to account for displacements between instruments.
   - Humidity correction of sonic temperature: Correction of air temperature estimated via sonic temperature was made to account the effects of humidity. This includes mean temperature values as well as any covariance (and related fluxes) that include sonic temperature.
   - Frequency response corrections: Application of corrects to account for signal attenuation due to sensor separation, path averaging, and finite instrument response times, using model-based spectral correction methods.
   - WPL correction for the air density fluctuations by Webb et al. (1980): Concentrations were corrected for variations in temperature and humidity for all measured gas concentrations.
   - Detrending: Removal of low-frequency trends from high-frequency wind and scalar time series prior to covariance calculation.

   In addition to corrections made in EddyPro, the following corrections and filters were applied to the processed EC data prior to completing emissions calculations:
   - Molar mass: Corrected fluxes output by EddyPro on a gas mole basis were converted to a carbon mass basis.
   - Removal of negative fluxes: Negative fluxes greater than -1 g $CO_2/m^2/h$ were set equal to zero. Negative fluxes less than or equal to -1 g $CO_2/m^2/h$ were excluded from the analysis. The adjustment is the result of a conservative assumption that the reservoir surface is not expected to act as a carbon sink at any point during the monitoring period. This assumption is supported by previous studies on reservoir GHG emissions (Teodoru et al., 2012, Deemer et al., 2016, Prairie et al., 2018).
   - Wind direction filter: Fluxes from outside angles described in Section 3.1 were excluded from the analysis.

- Signal strength filter: Fluxes from periods with low instrument signal strength (as indicated by the Received Signal Strength Indicator [RSSI] value), defined as less than 60 for the CO_2 analyzer sensor path and less than 20 for the CH_4 analyzer sensor path, were excluded from the analysis.
- Percentile filter: CO_2 fluxes exceeding the 95th percentile were excluded from the analysis.

2. Flux Chamber Measurements – Since the measurements were conducted in static mode, flux calculations are based on the cumulative mass of GHG measured by the analyzer over the measurement period per area isolated within the chamber. This approach produces a normalized emission flux since continuous homogeneous emissions are not expected from the reservoir area. The specific calculation methodology is from Measurement of Gaseous Emission rates from Land Surfaces using an Emission Isolation Flux Chamber, Kienbusch (1986).
3. Dissolved Carbon Concentration Measurements – This method provides a conservative estimate of emissions by comparing data points from nearby locations. The difference in dissolved carbon concentrations is used with water volumetric flow rates to determine a carbon mass balance. All decreases in carbon across the dam are conservatively allocated to CO_2 emissions.

3.5 Cumulative Emissions

Cumulative emissions were calculated by integrating flux chamber and EC data to determine a daily flux rate for each segment, multiplying those flux rates by the area of each segment and number of days in the month, and adding degassing emissions.

EC data established the relationship between daytime fluxes and nighttime fluxes. For a given month, EC data processed in 30-minute increments was averaged for each hour of the day to determine average temporal variation in a 24-hour period. Next, monthly sunrise and sunset times were considered to categorize each hour as daytime or nighttime. Average fluxes were then determined for daytime and nighttime, providing quantification of diurnal flux variation. The average daytime and nighttime fluxes for each EC station were then averaged, providing one value for average daytime flux from EC data and one value for average nighttime flux from EC data.

Flux chamber data established the spatial variation in fluxes across the segments of the reservoir. To integrate this with the temporal variation in EC data, different methods were used to calculate daytime and nighttime fluxes at the segment-level. For daytime fluxes, the flux chamber measured flux value was multiplied by the average number of daytime hours per day for the month, which was determined using mid-month sunrise and sunset times. For nighttime fluxes, the flux chamber measured flux value was multiplied by the ratio of average nighttime flux to average daytime flux, scaling the daytime measured value. This scaled flux was then multiplied by the number of nighttime hours per day for the month. The two resulting fluxes were added together, providing a daily flux value for each segment.

3.6 QA/QC Protocols

Quality Assurance/Quality Control (QA/QC) protocols were implemented to enhance transparency, consistency, comparability, completeness, and confidence in the GHG monitoring program. These procedures included:

- Instrument operation and calibration requirements, with instrumentation inspected monthly, and EC gas analyzers calibrated twice per year during seasonal changes.
- Sample preparation and handling protocols to prevent contamination and deterioration, which were followed by the third parties who completed sampling.
- Replicate measurements to ensure data reliability.
- Laboratory internal controls.
- Comprehensive data validation processes, including monthly reviews of data and emissions calculations.

Regular accuracy checks were conducted on data acquisition, measurement methods, calculations, uncertainty assessments, data management, and reporting procedures. Quality assurance measures helped ensure that all procedures align with study objectives.

3.7 System Maintenance

GHG monitoring equipment is maintained in accordance with vendor guidelines and equipment specifications. GHD personnel visited the site approximately once per month to perform routine maintenance. EC gas analysers were calibrated biannually, with calibration events corresponding with seasonal changes between winter and summer. Adhering to effective maintenance procedures and schedules will help ensure system longevity, high data quality, and data completeness.

4. Results and Discussion

4.1 Operational Assessment Results

4.1.1 Eddy Covariance

The annual wind roses and footprints for each EC station are presented below as Figure 4.1 through Figure 4.4. Both EC stations were placed to ensure that the prevailing wind directions allowed for flux measurement from the reservoir.

Daily temporal variation in average hourly CO_2 and CH_4 flux measured at each EC station is presented in Figure 4.5 and Figure 4.6.

At both EC stations, CO_2, which contributes the vast majority of CO_2e emissions, demonstrates a consistent diurnal trend. CO_2 flux is greatest later at night, around 00:00 to 06:00. It then decreases sharply during sunrise hours, continuing to decrease until the mid to late afternoon, between 15:00 and 17:00. CO_2 flux increases sharply during the evening, between 19:00 and 21:00, reaching an approximate maximum at 00:00. The diurnal flux variation captured by the EC stations is incorporated into cumulative emissions calculations, as described in Section 3.

In contrast to CO_2 flux, CH_4 flux did not exhibit a clear diurnal trend, particularly when considering both EC systems. At Site C, CH_4 flux was greatest at 02:00 and 07:00, was approximately average throughout the day, then decreased in the evening. At Bear Flat, CH_4 flux was greatest from 12:00 to 15:00, decreasing around sunset hours and holding at a minimum from around 02:00 to 05:00.

On an hourly basis, minimum, and average CO_2 flux was slightly greater at Site C (26.22, and 64.09 mg C/m^2/h respectively) than at Bear Flat (16.71 and 60.24 mg C/m^2/h respectively), while maximum CO_2 flux was comparable (110.93 and 111.37 mg C/m^2/h at Site C and Bear Flat). As Site C is downstream of Bear Flat, greater CO_2 flux could be due to greater dissolved CO_2 resulting in greater diffusive emissions. Additionally, the Site C EC footprint included the spillways and turbines, resulting in the EC station occasionally capturing degassing emissions.

Contrastingly, maximum and average CH_4 flux was lesser at Site C (0.217 and 0.125 C/m^2/h) than at Bear Flat (0.422 and 0.174 C/m^2/h). The greater CH_4 flux at Bear Flat may be the result of methanogenesis occurring nearby. The area around Bear Flat included wetlands and croplands pre-impoundment, neither of which were present to the same extent near Site C. A significant portion of the submerged organic material from these ecosystem types would undergo anaerobic decomposition, with CH_4 released as a product. The much lower solubility in water of CH_4 compared to CO_2 results in CH_4 being emitted closer to the source, including through ebullition. GHD personnel observed ebullition near Bear Flat during summer 2025, with measured flux chamber CH_4 concentrations exceeding 100,000 ppb prior to saturation of the gas analyzer. These observations support the elevated CH_4 flux measured at Bear Flat.

Annual temporal variation in average hourly CO_2 and CH_4 flux measured at each EC station is presented in Figure 4.7 and Figure 4.8.

At both EC stations, CO_2 flux was generally the greatest over summer, peaking June through August. At Site C, CO_2 flux tapered in September, then slowly increased throughout autumn, reaching a maximum in December, then dropping to a minimum in March. This trend was not reflected at Bear Flat, where CO_2 flux decreased sharply from

October to November and remained low in December and March. It should be noted that a hardware failure limited Bear Flat EC data collection to only the last week of November, and that extreme cold limited both systems to only the first week of December. Previous studies have consistently found GHG flux from reservoirs to be greatest in the spring and summer, and lowest in the winter. The departure from this trend observed at Site C, particularly in the month of December, may be the result of an insufficient sample size or may be influenced by the lack of ice cover at the dam and degassing emissions being included in the EC footprint.

CH_4 flux demonstrated a more consistent trend between the two EC stations. At both, flux peaked during warmer months, namely July. CH_4 flux then decreased sharply in autumn, being near minimum in November and December. At Site C, CH_4 flux had increased back to autumn levels in March. Once again, it is worth noting the limited data availability in November and December, as well as additional months with limited data. At Site C, CH_4 flux data was unavailable for June, and at Bear Flat, CH_4 flux data was unavailable for April, June, September, October, and March. Instrument errors were the primary cause of limited data availability.

EC sample sizes were generally good on an hourly basis, but more limited monthly. Table 4.1 and Table 4.2 present EC data availability at each station, after filtering for wind direction.

While both EC stations have combustion sources nearby (heavy equipment activities at Site C and highway traffic at Bear Flat), the wind direction filter applied to the EC data should generally exclude any CO_2 emissions from combustion or unburned CH_4. The potential for non-reservoir anthropogenic GHG emissions to impact the EC measurements is greater at Site C than at Bear Flat.

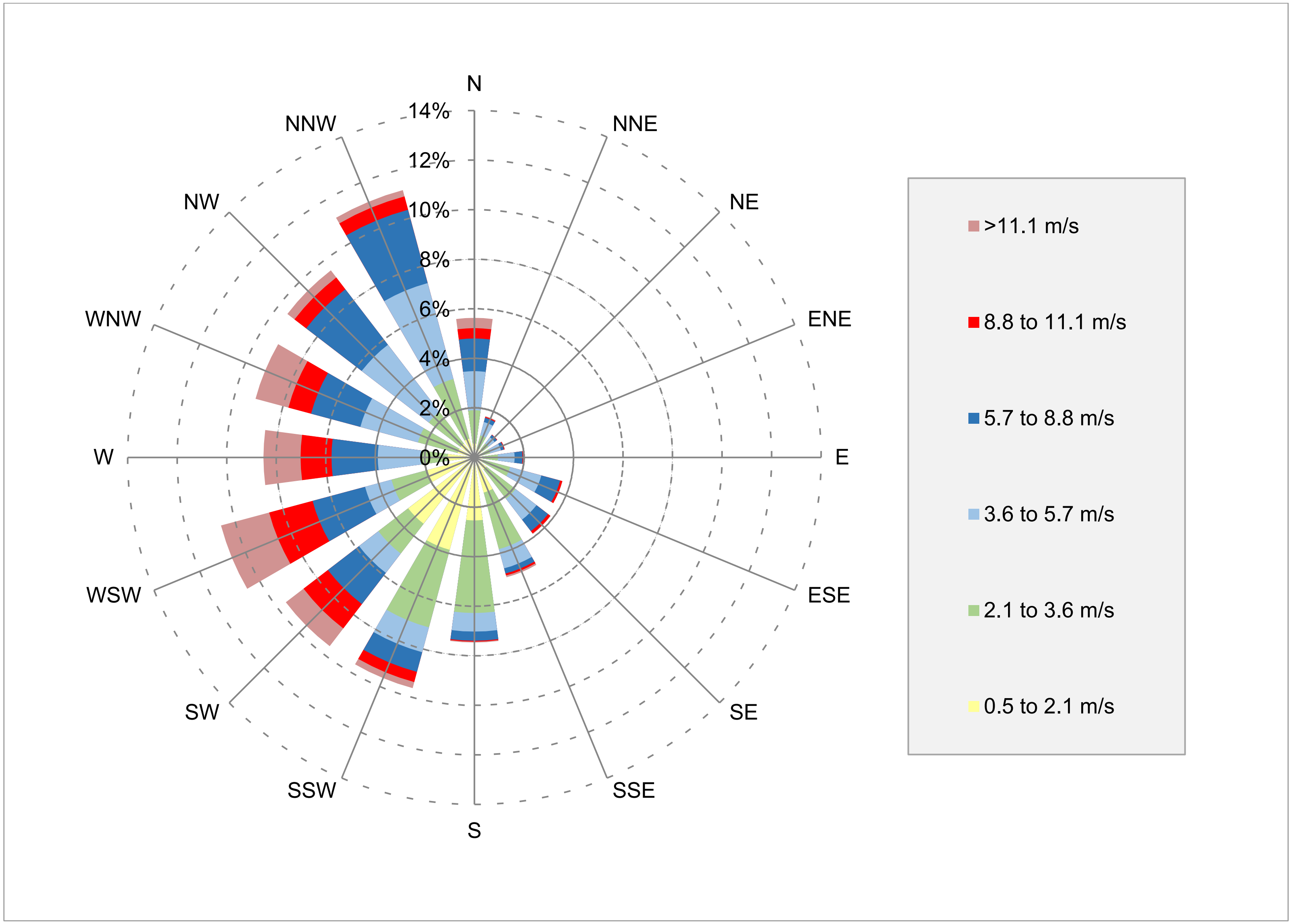

Figure 4.1 Annual wind rose – Site C EC system – April 2025 to March 2026

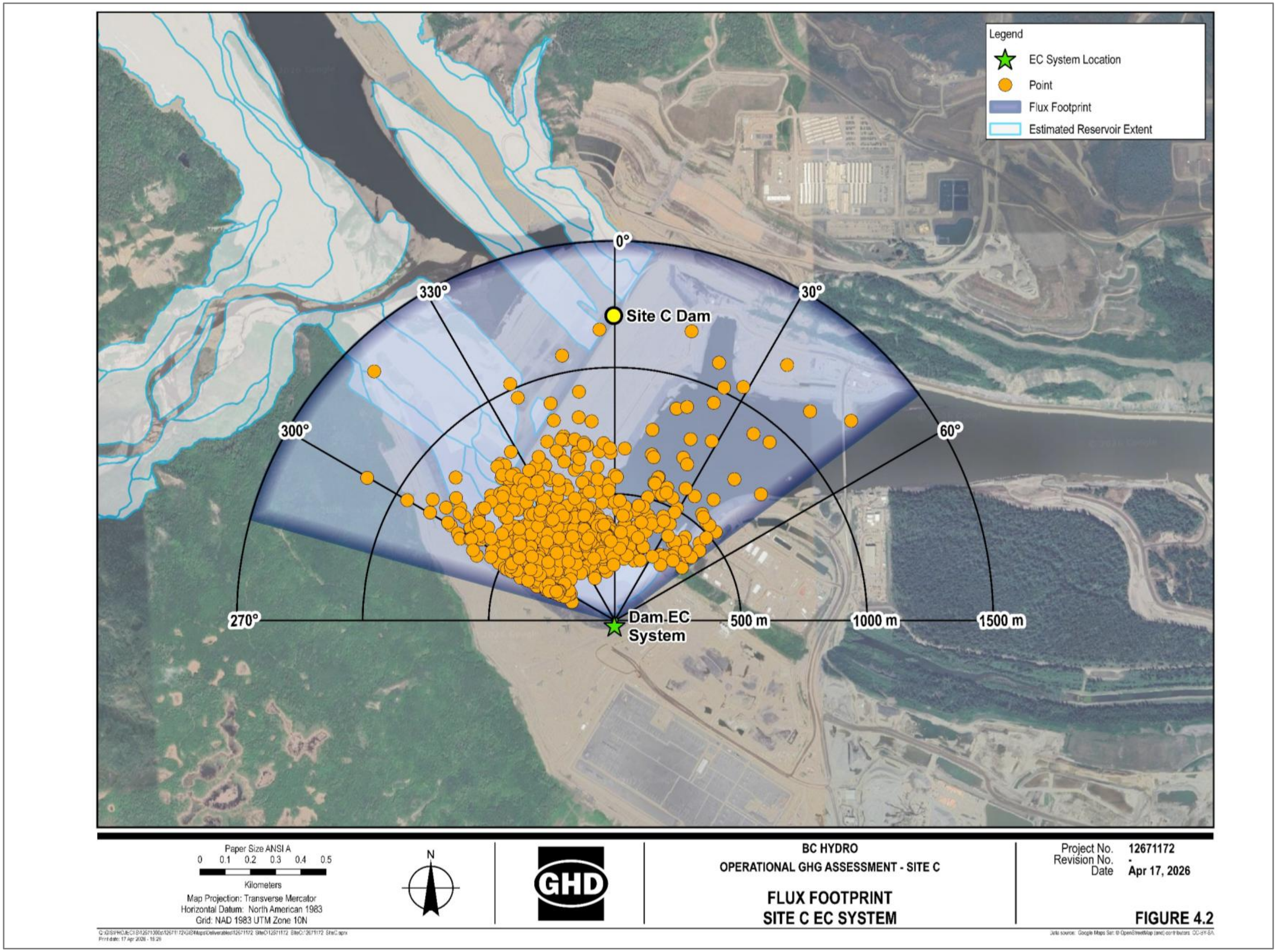

Figure 4.2 Flux footprint – Site C EC system – April 2025 to March 2026

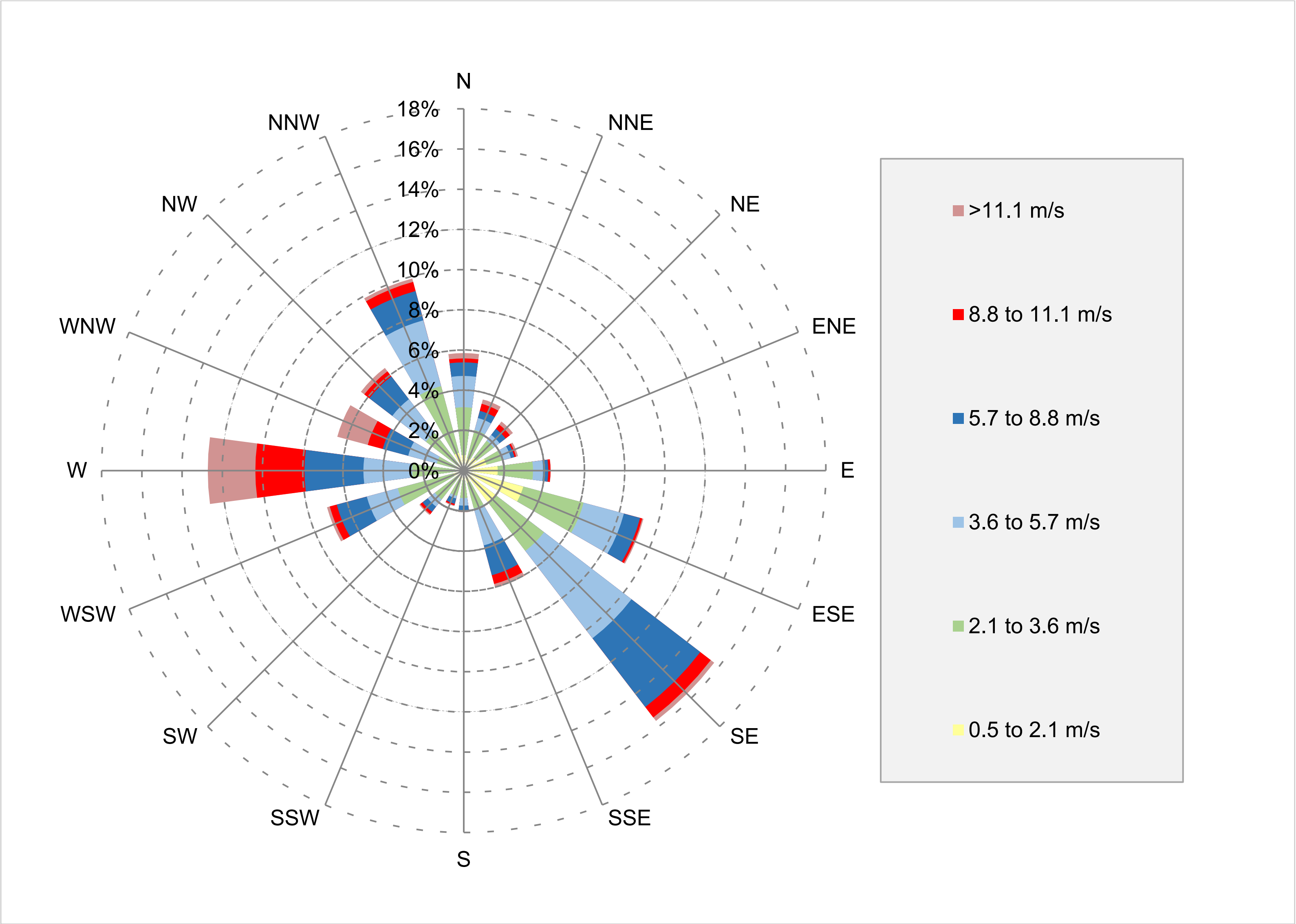

Figure 4.3 ***Annual wind rose – Bear Flat EC system – April 2025 to March 2026***

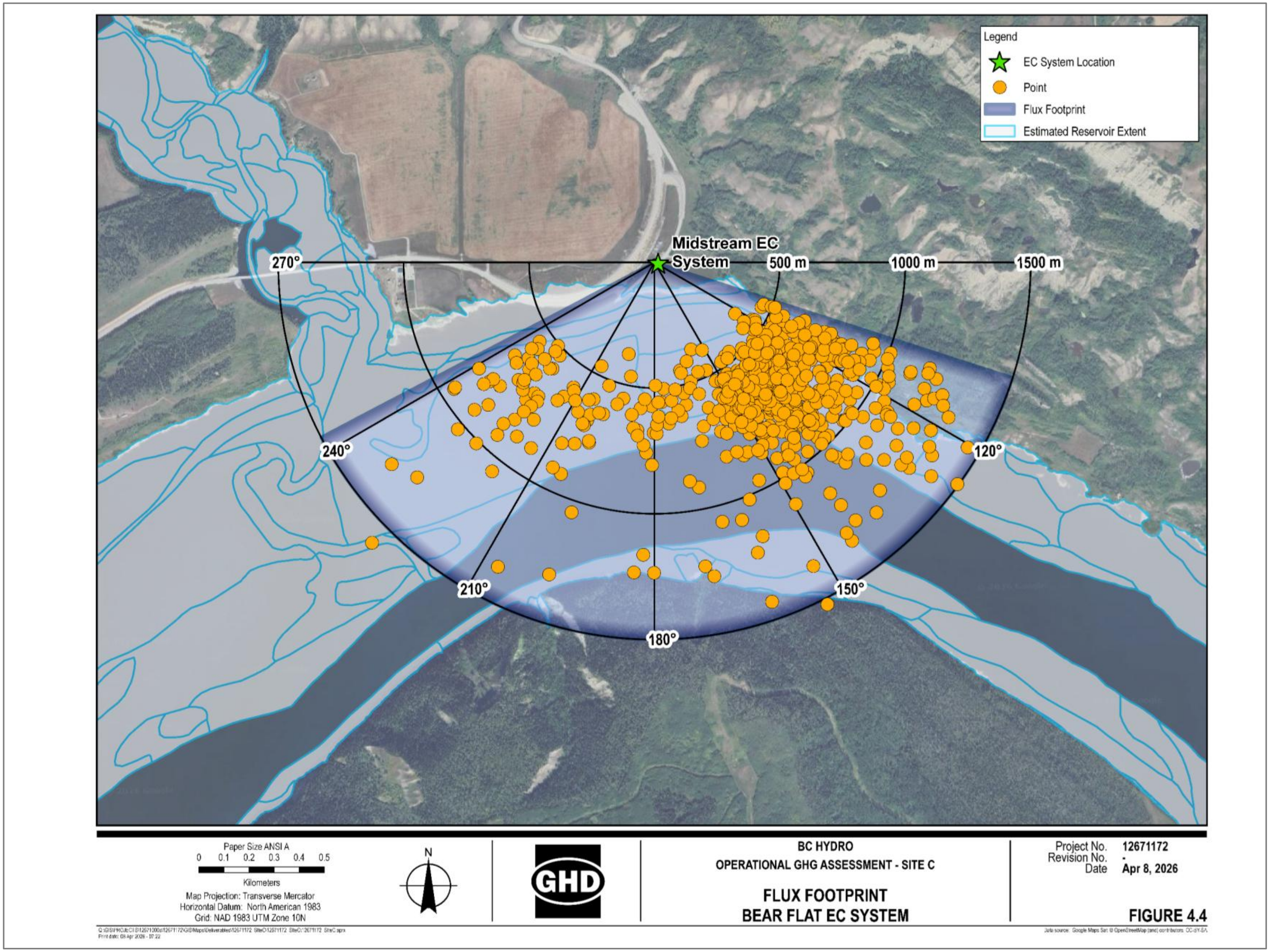

Figure 4.4 Flux footprint – Bear Flat EC system – April 2025 to March 2026

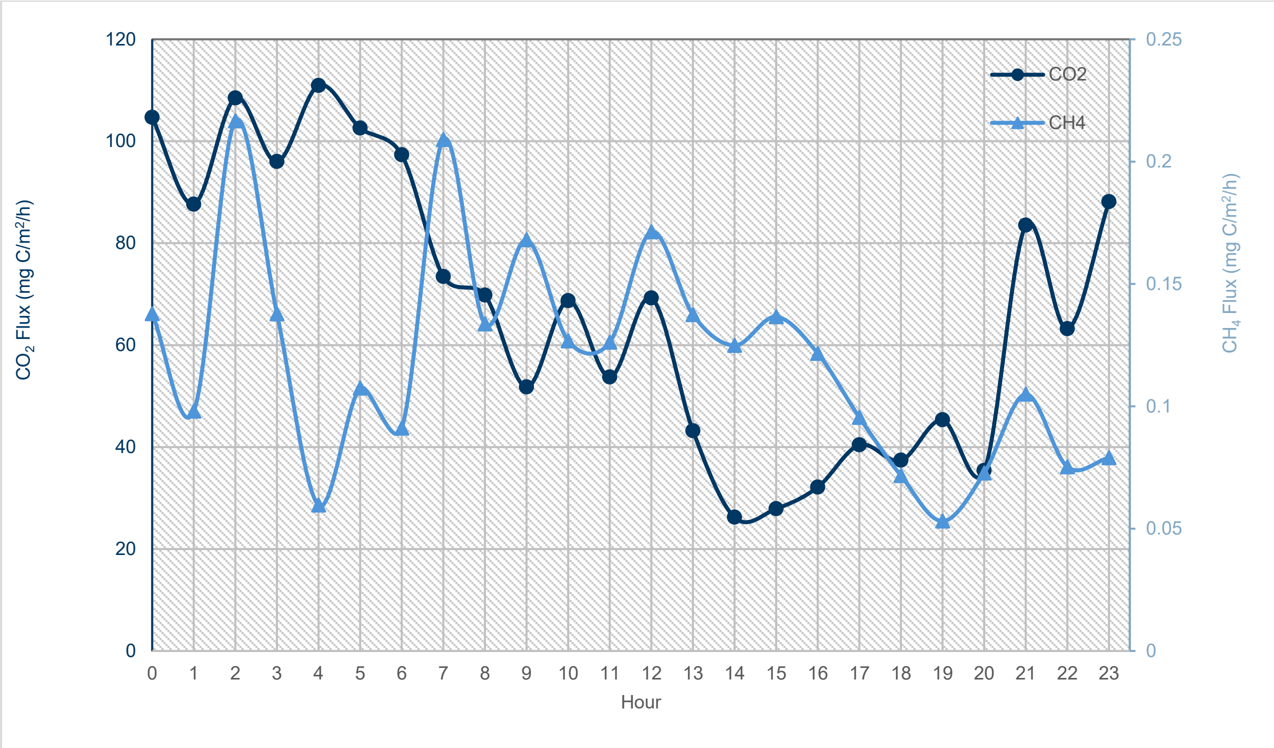

Figure 4.5 CO_2 and CH_4 daily temporal variation – Site C EC system

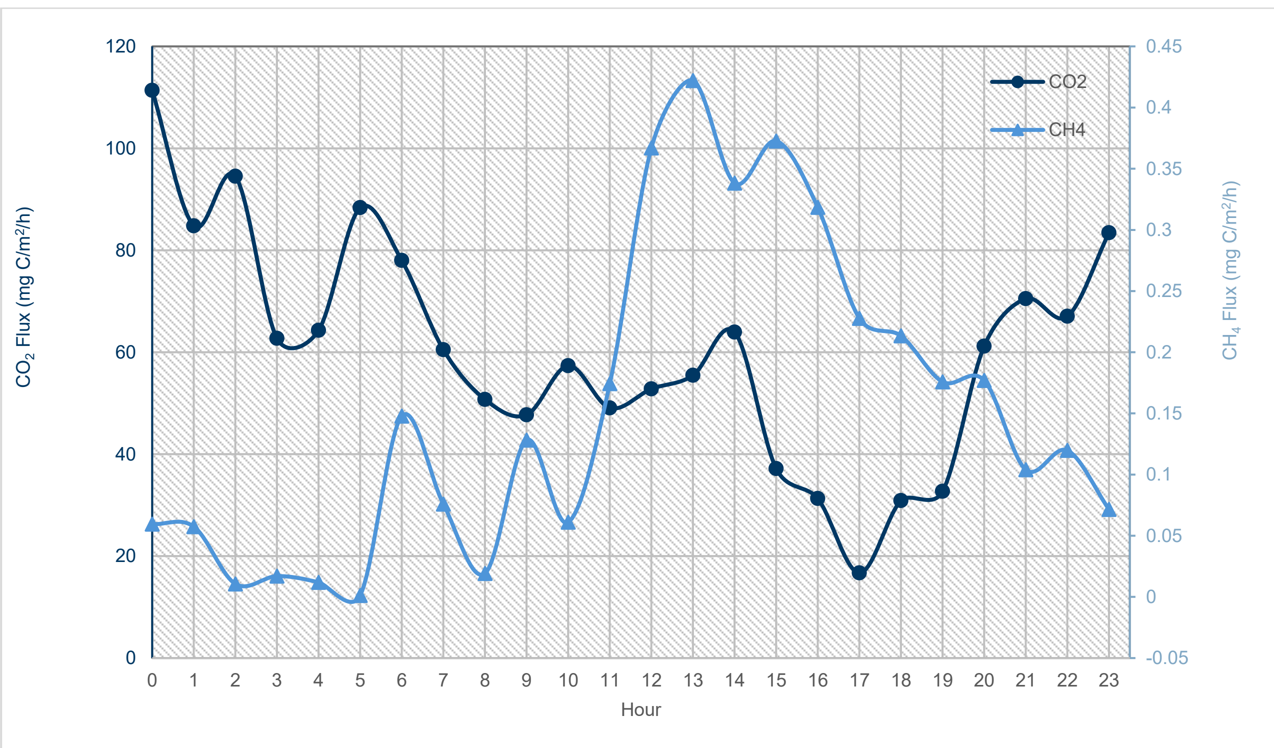

Figure 4.6 CO_2 and CH_4 daily temporal variation – Bear Flat EC system

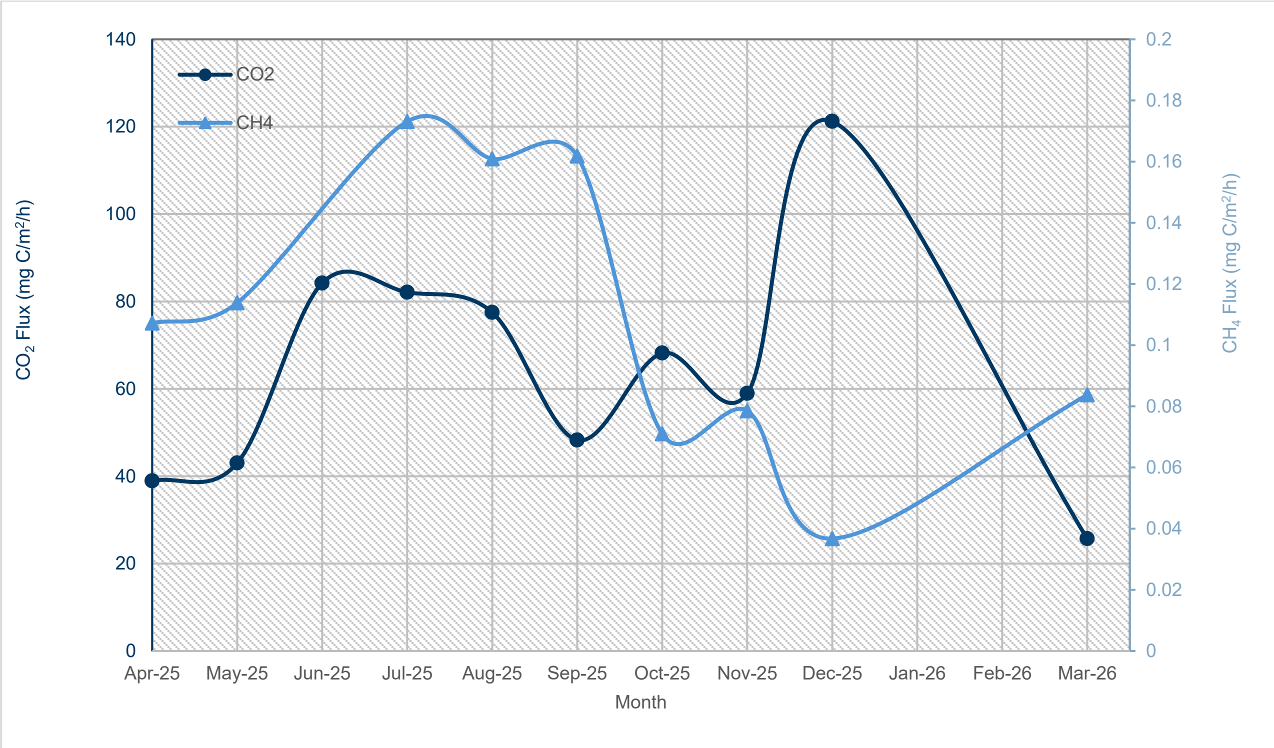

Figure 4.7 CO_2 and CH_4 annual temporal variation – Site C EC system

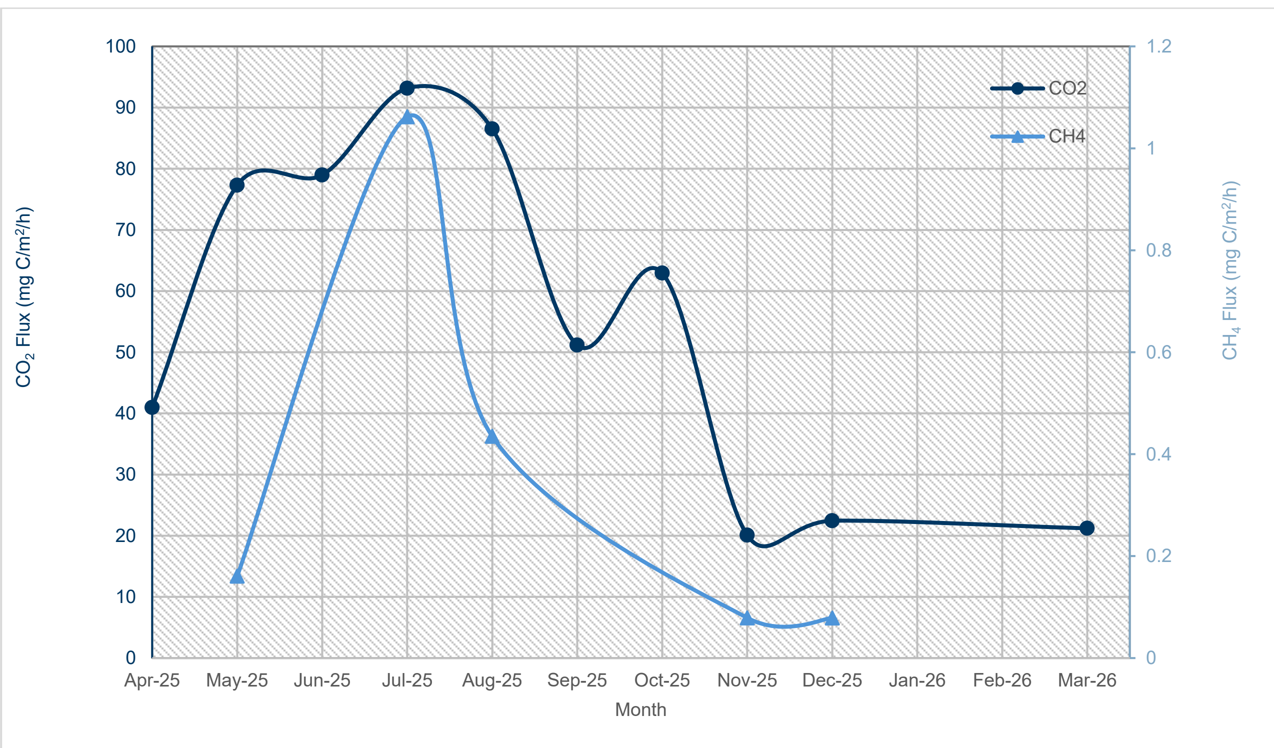

Figure 4.8 CO_2 and CH_4 annual temporal variation – Bear Flat EC system

Table 4.1 Hourly EC Data Availability

Hour	Number of valid 30-minute CO_2 flux measurements		Number of valid 30-minute CH_4 flux measurements	
	Site C	Bear Flat	Site C	Bear Flat
0	88	138	53	22
1	99	139	58	24
2	114	147	70	20
3	110	117	72	15
4	106	108	73	13
5	114	93	77	9
6	122	115	71	12
7	154	100	84	10
8	179	124	108	12
9	195	125	117	12
10	186	119	116	14
11	194	113	125	17
12	182	137	110	22
13	188	133	121	22
14	171	125	113	16
15	155	124	110	17
16	158	122	102	23
17	134	145	88	23
18	113	154	70	24
19	87	135	51	13
20	83	130	51	17
21	80	140	52	18
22	71	143	48	20
23	86	131	54	18
Total	**3169**	**3057**	**1994**	**413**

Table 4.2 Monthly EC Data Availability

Month	Number of valid 30-minute CO_2 flux measurements		Number of valid 30-minute CH_4 flux measurements	
	Site C	**Bear Flat**	**Site C**	**Bear Flat**
Apr-25	124	196	121	0
May-25	271	164	193	134
Jun-25	461	308	0	1
Jul-25	530	388	110	110
Aug-25	591	458	557	22
Sep-25	357	548	310	0
Oct-25	296	340	172	0
Nov-25	193	63	189	62
Dec-25	25	89	22	84
Jan-25	0	0	0	0
Feb-25	0	0	0	0
Mar-25	324	503	322	0
Total	**3169**	**3057**	**1994**	**413**

4.1.2 Flux Chamber

A total of 149 valid flux chamber samples were taken during the monitoring period. Samples were taken monthly in segments which were accessible and free of ice. Table 4.3 summarizes the number of samples collected across each segment and each month. Figure 3.5 illustrates the segment locations.

Table 4.3 Number of Valid Flux Chamber Measurements per Segment and per Month

Month	Segment ID													
	A	B	C	D	E	F	G	H	I	J	K	L	M	Sum
Apr-25	2	1	1	0	0	0	4	2	1	1	1	1	1	15
May-25	2	1	2	0	0	0	3	2	1	1	1	1	1	15
Jun-25	2	1	2	0	0	0	3	2	0	1	1	1	1	14
Jul-25	2	1	1	0	0	0	2	2	1	1	1	2	1	14
Aug-25	2	1	2	0	0	0	6	3	1	1	2	3	1	22
Sep-25	2	1	2	0	0	0	3	3	2	2	4	2	2	23
Oct-25	2	1	1	0	0	0	2	4	2	1	3	1	1	18
Nov-25	2	1	2	0	0	0	4	3	1	1	1	1	1	17
Dec-25	1	1	0	0	0	0	0	0	0	0	0	0	1	3
Jan-26	0	0	0	0	0	0	0	0	0	0	0	0	0	0
Feb-26	0	0	0	0	0	0	0	0	0	0	0	0	0	0
Mar-26	2	2	0	0	0	0	0	0	0	0	0	2	2	8
Sum	19	11	13	0	0	0	27	21	9	9	14	14	12	149

Segment A is located ~50 km downstream of the dam and is sampled for comparison to baseline levels. Previous studies have found that downstream diffusive emissions return to baseline levels within the first 50 km downstream of a reservoir. Flux chamber results from Segment A have been generally consistent with baseline flux measurements from the Peace River. These results are presented below in Table 4.4. For comparison, the baseline flux from the Peace River and tributaries ranged from 749.8 to 4,427 mg C/m^2/d for CO_2 and 0.04 to 11.1 mg C/m^2/d for CH_4.

Table 4.4 Monthly Fluxes in Segment A

Month	CO_2 Flux (mg C/m^2/d)	CH_4 Flux (mg C/m^2/d)
Apr-25	2,970	1.02
May-25	4,891	9.47
Jun-25	3,593	6.14
Jul-25	5,155	17.64
Aug-25	4,900	35.56
Sep-25	5,312	8.46
Oct-25	3,825	15.47
Nov-25	2,134	1.39
Dec-25	4,073	14.09
Jan-26	2,723	1.49
Feb-26	2,621	1.43
Mar-26	2,018	1.10
Average	3,685	9.44

As shown above, while the average CO_2 and CH_4 flux were within the baseline ranges, both were towards the upper bound of the baseline. Measured CO_2 fluxes exceeded the baseline range in July, August, and September, while measured CH_4 fluxes exceeded the baseline range for July, August, October, and December. January and February fluxes were estimated using measurements taken in March, which were within the baseline range. The high average fluxes and multiple months of exceedances potentially imply elevated diffusive emissions 50 km downstream of the dam.

Opposing the potential of elevated diffusive emissions 50 km downstream of the dam is the disconnect between fluxes measured immediately downstream and 50 km downstream. A comparison of these fluxes can be found in Figure 4.9 and Figure 4.10.

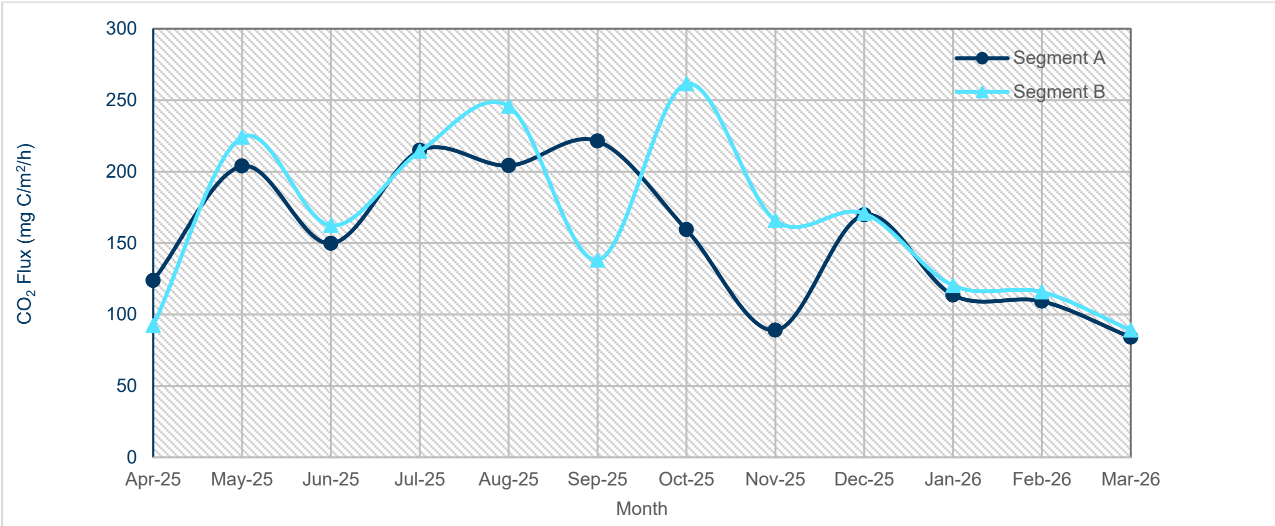

Figure 4.9 Comparison of measured CO_2 flux between Segment A and Segment B

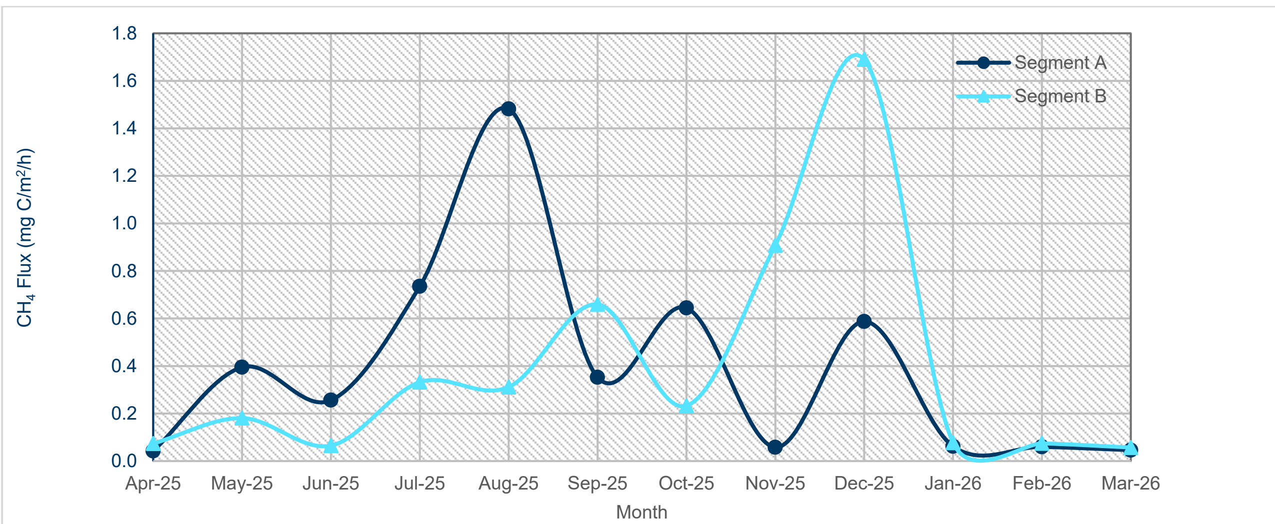

Figure 4.10 Comparison of measured CH_4 flux between Segment A and Segment B

For April through July, both CO_2 and CH_4 fluxes at Segment A and Segment B generally trended together. This ended in August, when CO_2 flux decreased slightly in Segment A while increasing in Segment B. The inverse occurred in September, when CO_2 flux increased in Segment A, and decreased sharply in Segment B. Flux trends once again inverted in October, and CO_2 flux in the two segments remained disconnected until December. From December on, CO_2 fluxes in the two segments trended closely.

Meanwhile, CH_4 fluxes demonstrated a similar disconnect, with CH_4 flux decreasing slightly in August in Segment A, while increasing dramatically in Segment B. CH_4 flux continued to trend inversely in following months, most notably with Segment B CH_4 flux at a monthly maximum in December and Segment A CH_4 flux relatively average. CH_4 fluxes in both segments were comparable and very low in March, with those results also applied to January and February.

The breakdown of the trend between Segment A and Segment B fluxes from August onwards suggests that an unknown factor between the dam and Segment A is potentially impacting Segment A fluxes, such as land use/ecosystem-related seasonal carbon variation. Alternatively, the differences in measured fluxes between the two segments could be noise. Generally, two flux chamber measurements were taken in Segment A and one in Segment B each month. Given the disconnect between measured fluxes in the two segments, and the limited number of samples, there is hesitation in attributing increased fluxes in Segment A to the dam.

Segments D, E, and F are located between the dam and Bear Flat and are not accessible from public or BC Hydro-owned roads. As a result, instead of conducting flux chamber measurements, the average of the monthly fluxes in the segments immediately upstream and downstream of D, E, and F were used for emissions calculations.

Fluxes for the remaining segments are presented under cumulative emissions.

4.1.3 Dissolved Carbon

Water quality sampling was conducted at locations near upstream and near downstream of the dam as described in Section 3. To calculate degassing emissions, the difference in DIC (measured in mg/L) from upstream to downstream of the dam was multiplied by the monthly volumetric flow of water, returning a mass change of carbon. As the measure being used was dissolved inorganic carbon, which is a measure of CO_2 and carbonate concentrations, the entire reduction in carbon was conservatively allocated to CO_2 emissions.

Optimally, dissolved CO_2 concentrations would have been measured immediately upstream and downstream of the dam, and these values would have been used to quantify degassing emissions (UNESCO/IHA, 2010). The available water sampling data did not include measures of dissolved gases, and safety concerns accessing the reservoir above and river below the dam prohibited additional sampling from being completed. The use of DIC for degassing calculations is more conservative, as any decreases in dissolved carbonates would be attributed to CO_2 emissions. Changes in dissolved carbonates as water passes through the dam are also expected to be minimal, as there is no specific mechanism that would add or remove a significant amount of carbonate from the water.

During the calculation of degassing emissions, it was identified that monthly DIC concentrations varied markedly, particularly downstream of the dam. Upstream, DIC ranged from 20.80 to 24.70 mg C/l, while downstream, DIC ranged from 17.20 to 24.30 mg C/l. Even more notably, the difference between DIC upstream and downstream ranged from -0.50 mg C/l in November, to 3.60 mg C/l in October, with a negative value indicating an increase in carbon across the dam. The high variability without a clear cause or seasonal trend reduced confidence in the results of individual water samples. As a result, the average of all water samples taken at each location was used for degassing calculations, with monthly variation in calculated degassing emissions solely the result of changes in water throughput.

For monthly water discharge, the greater of the downstream hydrometric station discharge rates and the BC Hydro-supplied turbine throughput rates were used as the turbine throughput rate excludes spillways, while the hydrometric station discharge rate was found to be less than the turbine throughput rate for one month of the year. The use of the greater monthly flow rate for calculation of degassing emissions is conservative.

Monthly degassing emissions, calculated using dissolved carbon concentrations, are presented below in Figure 4.11.

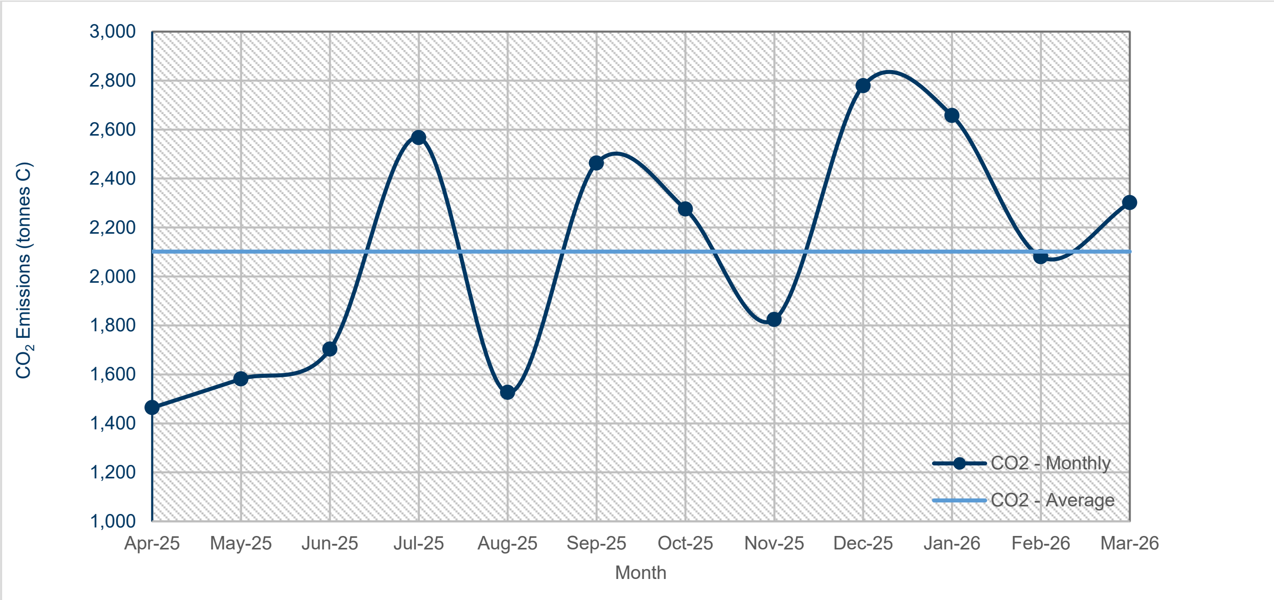

Figure 4.11 Monthly degassing emissions

4.2 Cumulative Emissions

Cumulative emissions were calculated by integrating flux chamber and EC data as described in Section 3. Calculations were done for each segment monthly, with total monthly emissions being the sum of each segment's emissions and the degassing emissions. Monthly emissions by segment are shown below in Figure 4.12 and Figure 4.13.

For the purposes of cumulative emissions calculations, outliers in monthly CO_2 and CH_4 flux by segment were included. Eddy covariance and flux chamber results used to calculate monthly CO_2 and CH_4 flux by segment were determined to be valid as described throughout Section 3. Excluding outliers based on statistics alone was determined to be unreasonable due to the potential of measurements with high flux values reflecting real, episodic processes. While the inclusion of outliers may be conservative, the exclusion would introduce a downward bias in cumulative emissions.

In total, GHD quantified 531,862 tonnes CO_2e of GHG emissions from the Site C reservoir during the monitoring period. CO_2e was calculated using the Intergovernmental Panel on Climate Change (IPCC) Fifth Assessment Report (AR5) global warming potential (GWP) values of 1 for CO_2 and 28 for CH_4 (IPCC, 2014), as adopted by BC.

In general, CO_2 flux was greater closer to the dam, decreasing while moving up-reservoir. The exceptions to this are Segment H and Segment I. These two segments are located immediately downstream and upstream, respectively, of where the Halfway River flows into the reservoir. Both segments included wetlands as a pre-impoundment ecosystem type. Flux chamber measurements for both segments are taken near the Halfway River, in some cases directly over a pre-impoundment river delta-like area. These segment's proximity to the Halfway River, and the carbon-rich pre-impoundment ecosystem types are both potential factors contributing to the elevated fluxes observed.

Unlike CO_2, CH_4 flux did not have an apparent trend relative to segment distance from the dam. Once again, Segment H and Segment I had elevated CH_4 fluxes relative to their neighbouring segments. The Halfway River and carbon-rich pre-impoundment ecosystem types are again potential contributing factors for the elevated fluxes. The lower solubility of CH_4 in water compared to CO_2 is also a likely contributing factor, with CH_4 emissions expected to be more localized to the organic carbon source. Segment K also had elevated CH_4 flux, despite having a CO_2 flux which followed the distance-from-dam trend. The different properties and processes of CO_2 and CH_4 mean that a similar trend between the two is not necessarily expected.

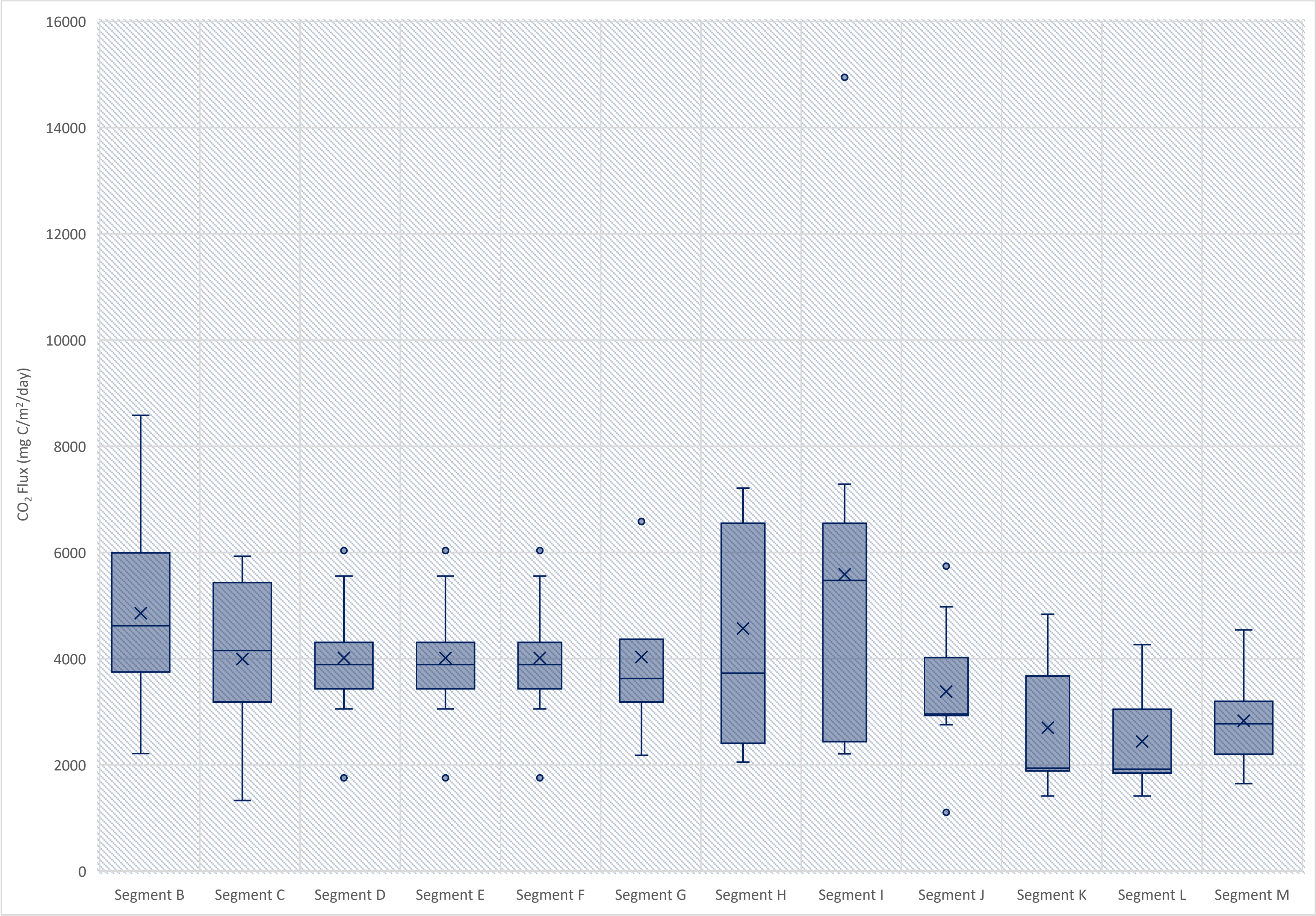

Figure 4.12 CO_2 flux by segment

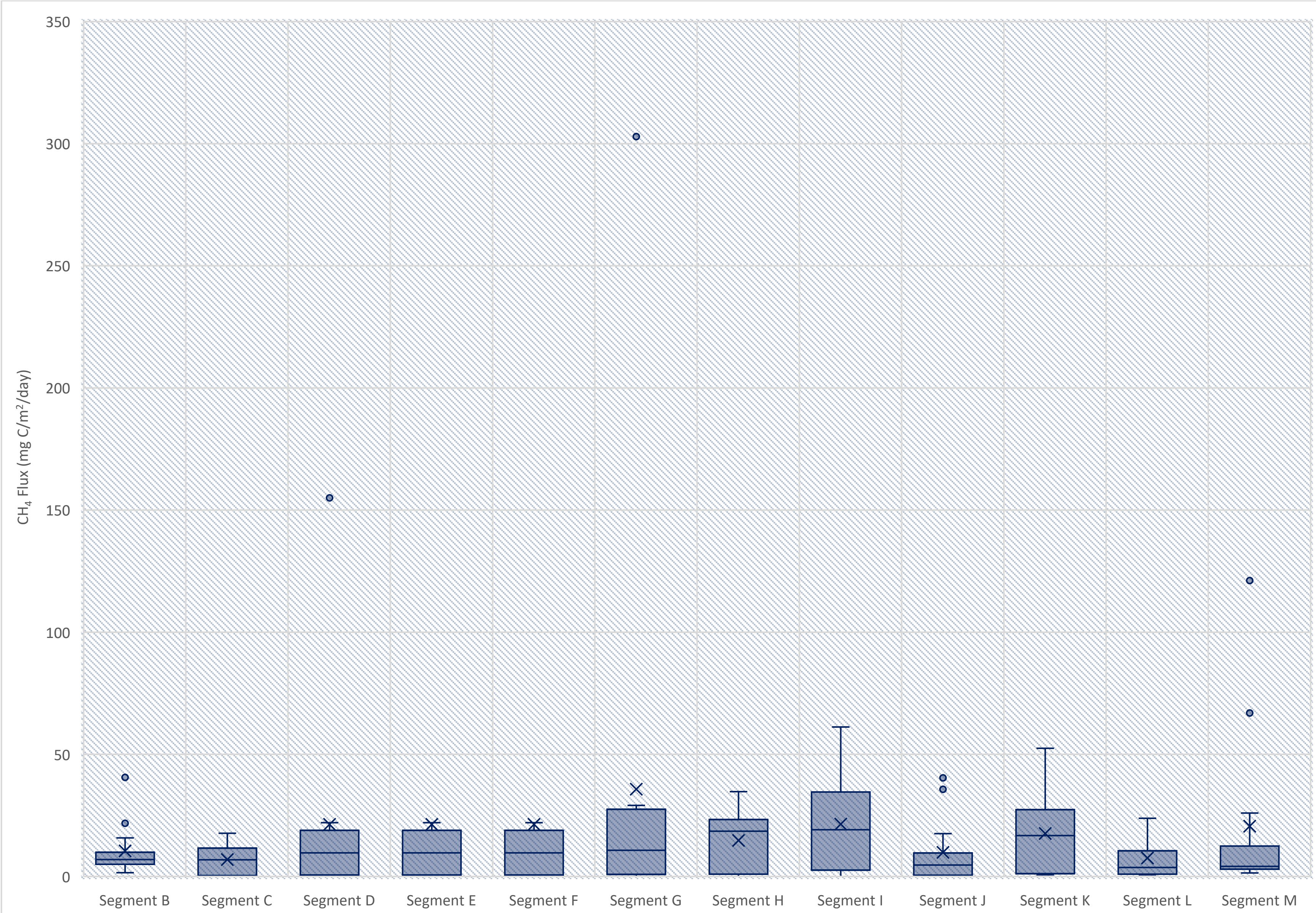

Figure 4.13 ***CH_4 flux by segment***

The above presented fluxes were used with degassing emissions and ice cover (for winter months) to calculate monthly and cumulative emissions. Figure 4.14 presents the cumulative emissions for the first monitoring year.

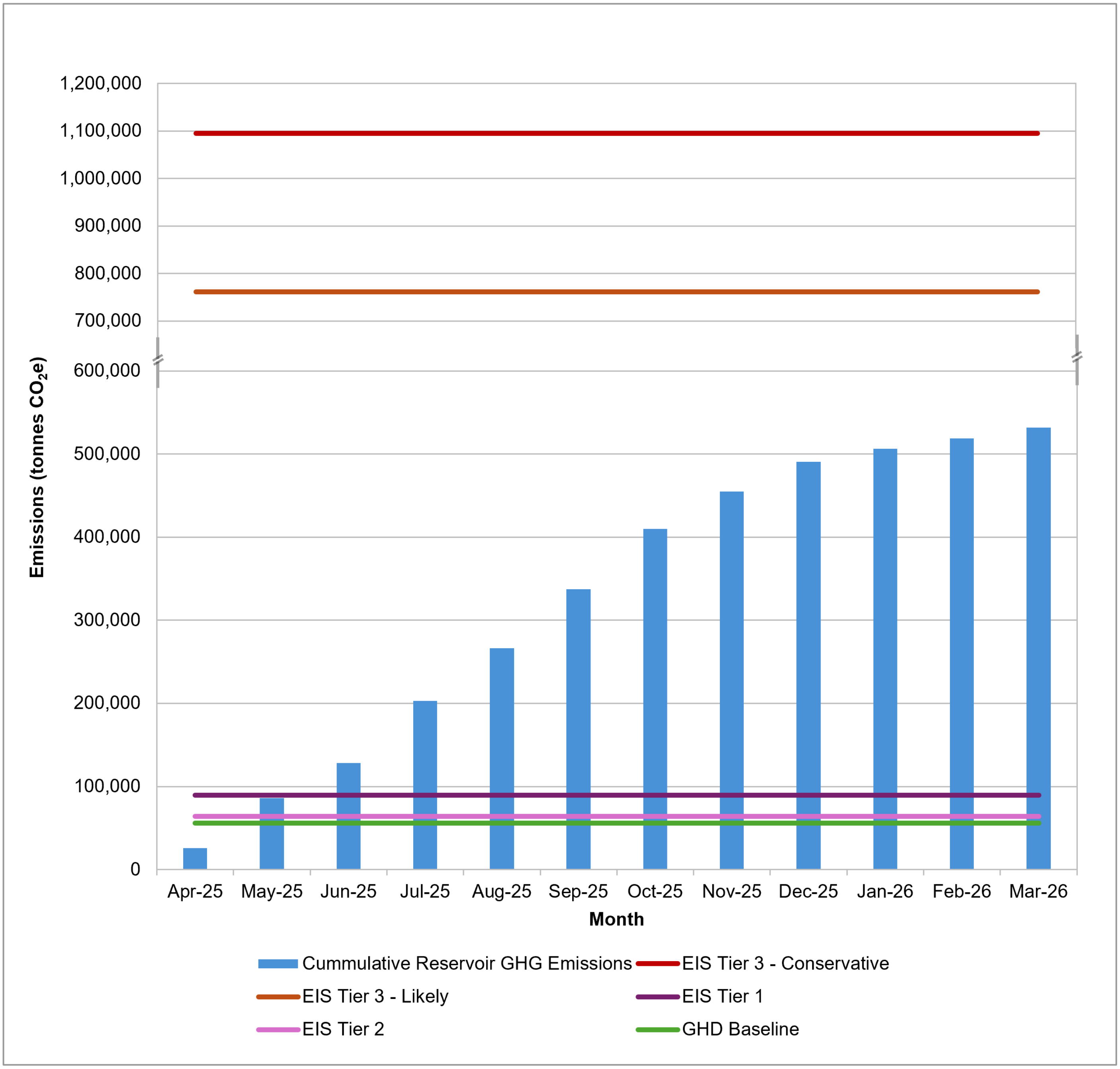

Figure 4.14 ***Cumulative reservoir GHG emissions, first monitoring year***

As shown in the figure, the first year of GHG emissions from the Site C reservoir greatly exceed the 2013 Environmental Impact Statement (EIS) Tier 1 and Tier 2 models, as well as the GHD Baseline. GHG emissions were lower than predicted by both the conservative and likely EIS Tier 3 models. The EIS models were prepared following methods described by the Intergovernmental Panel on Climate Change (IPCC, 2003). The Tier 1 and Tier 2 models used simple calculations to estimate emissions from land flooding only and land flooding and degassing, respectively. The Tier 3 model used a more detailed carbon model to account for the various stocks, processes, and fluxes relevant to hydroelectric reservoirs (BC Hydro, 2013, Stantec Consulting Ltd., 2012). Comparisons to the EIS models were completed based on total magnitude of emissions.

Tabulated emissions by month and by segment are provided in Appendix A.

4.3 Net Emissions

As part of the conclusion of the Baseline Assessment, GHD estimated total pre-impoundment GHG emissions to be 49,638 tonnes CO_2e. Subtracting the pre-impoundment emissions from the operational emissions yields net emissions of approximately **482,224 tonnes CO_2e** for the first year of operations.

4.4 Limitations

The results and interpretations presented in the Operational Assessment are subject to the following limitations, which should be considered when reviewing the findings.

- Monitoring Period and Data Completeness – The Operational Assessment represents an evaluation covering the period from 1 April 2025 to 31 March 2026. Data availability varied by monitoring method and month due to equipment downtime, environmental conditions, and site access constraints.

  Eddy covariance data availability was limited during certain periods as a result of instrument malfunctions and extreme cold weather conditions, particularly in late autumn and early winter. Where data gaps occurred, emissions calculations relied on fewer sample points, an approach considered reasonable given the role of eddy covariance data in characterizing temporal variability rather than absolute magnitude.
- Winter Conditions and Ice Cover – Flux chamber monitoring could not be conducted during periods when reservoir segments were ice-covered or otherwise inaccessible. For these periods, emissions from ice-covered areas were assumed to be negligible for the purposes of monthly and cumulative emissions calculations. Ice extent was estimated using a combination of satellite imagery and field observations. While this assumption is consistent with published literature on reservoir GHG emissions, it introduces uncertainty where localized emissions may persist beneath partial or transient ice cover. Additionally, buildup of dissolved or entrapped gases could be released over a short span as ice melts.
- Spatial Coverage and Segment Representation – Flux chamber measurements were conducted at discrete locations within defined reservoir segments. Exact sampling locations varied monthly based on site conditions and accessibility. For segments that were inaccessible from public or BC Hydro–owned roads (Segments D, E, and F), emissions were estimated using the average of fluxes measured in adjacent upstream and downstream segments. This interpolation approach assumes spatial continuity in emissions characteristics and may not fully capture localized variability within those segments.
- Ebullition Pathway Characterization – Ebullitive methane emissions were not quantified as a distinct emission pathway in this assessment. While ebullition contributes to the overall reservoir GHG budget, discrete bubbling events were not separately measured or partitioned. Instead, ebullitive emissions occurring within the eddy covariance footprint are implicitly included in the net flux measured by the eddy covariance systems. As a result, the relative contribution of ebullition to total emissions cannot be independently assessed.
- Downstream Diffusive Emissions – This assessment does not quantify downstream diffusive CO_2 and CH_4 emissions as a reach-scale emission pathway. Flux chamber measurements conducted approximately 50 km downstream of the dam (Segment A) are used for comparison with baseline conditions to assess whether downstream fluxes differ from pre-impoundment levels. However, these data are not extrapolated to estimate cumulative downstream diffusive emissions, and intermediate downstream reaches were not monitored due to logistical and environmental constraints.
- Degassing Emissions Estimation – Degassing emissions downstream of the dam were estimated using differences in DIC concentrations between upstream and downstream sampling locations combined with water discharge rates. This method conservatively attributes observed decreases in DIC to CO_2 emissions associated with turbine and spillway passage. Monthly DIC measurements exhibited high variability, including instances

where downstream concentrations exceeded upstream values. To address this variability, average DIC differences were applied across all months, which reduces sensitivity to anomalous samples but may obscure short-term variability in degassing processes.

- Treatment of Negative CO_2 Fluxes – Negative CO_2 fluxes measured by eddy covariance systems were evaluated as potential artifacts associated with low turbulence conditions and measurement uncertainty. To maintain a conservative emissions estimate, negative flux values within a defined threshold were set to zero, and more extreme negative values were excluded from averaging. This treatment reflects a reporting convention intended to avoid underestimation of emissions and does not preclude the possibility of short-duration net uptake under specific environmental conditions.
- Attribution of Emissions Drivers – Observed spatial and temporal variability in emissions reflects the influence of multiple interacting factors, including pre-impoundment land cover, organic matter availability, hydrology, temperature, and reservoir operations. While patterns in the data are discussed, definitive attribution of observed emissions to specific drivers, particularly downstream of the dam, is limited by data availability and confounding environmental influences.

5. References

BC Hydro, 2013. *Site C Clean Energy Project: Environmental Impact Statement*. Vancouver, BC: BC Hydro. Available at: https://www.iaac-aeic.gc.ca/050/evaluations/document/93686

Deemer, B.R., Harrison, J.A., Li, S., Beaulieu, J.J., DelSontro, T., Barros, N., Bezerra-Neto, J.F., Powers, S.M., Dos Santos, m.A., and Vonk, J.A., 2016. Greenhouse Gas Emissions from Reservoir Water Surfaces: A New Global Synthesis. *Bioscience*. 66(11), pp. 949-964. doi: 10.1093/biosci/biw117.

Demarty, M., and Tremblay, A., 2017. Long term follow-up of pCO_2, pCH_4 and emissions from Eastmain 1 boreal reservoir, and the Rupert diversion bays, Canada. Ecohydrology & Hydrobiology, 19. doi: 10.1016/j.ecohyd.2017.09.001

Gill Instruments, 2024. WindMaster Pro Datasheet. https://gillinstruments.com/wp-content/uploads/2022/08/WindMaster-Pro-iss-8.pdf

IPCC, 2014. Climate Change 2014: Synthesis Report. Contribution of Working Groups I, II and III to the Fifth Assessment Report of the Intergovernmental Panel on Climate Change. IPCC, Geneva, Switzerland.

International Hydropower Association, United Nations Educational, Scientific, and Cultural Organization (IHA/UNESCO). 2010. GHG Measurement Guidelines for Freshwater Reservoirs. IHA. (08 December 2022; https://www.hydropower.org/publications/ghg-measurement-guidelines-for-freshwater-reservoirs)

Jager, H.I., Griffiths, N.A., Hansen, C.H., King, A.W., Matson, P.G., Singh, D. and Pilla, R.M., 2022. Getting lost tracking the carbon footprint of hydropower. Renewable and Sustainable Energy Reviews, 162, p.112408.

Kienbusch, M.R., 1986. Measurement of gaseous emission rates from land surfaces using an emission isolation flux chamber. Environmental Monitoring Systems Laboratory, U.S. Environmental Protection Agency.

LI-COR Environmental, 2024. LI-7500DS Specifications. https://www.licor.com/env/products/eddy-covariance/LI-7500DS

LI-COR Environmental, 2024. LI-7700 Specifications. https://www.licor.com/env/products/eddy-covariance/LI-7700

Prairie, Y. T., Alm, J., Beaulieu, J., Barros, N., Battin, T., Cole, J., del Giorgio, P., Del Sontro, T., Guérin, F., Harby, A., Harrison, J., Mercier-Blais, S., Serça, D., Sobek, S., and Vachon, D., 2018. Greenhouse Gas Emissions from Freshwater Reservoirs: What Does the Atmosphere See? *Ecosystems*, 21(5), pp.1058–1071**.** https://doi-org.login.ezproxy.library.ualberta.ca/10.1007/s10021-017-0198-9

Province of British Columbia, 2013. B.C. field sampling manual. Government of British Columbia.

Rey-Sanchez, C., Arias-Ortiz, A., Kasak, K., Chu, H., Szutu, D., Verfaillie, J., and Baldocchi, D., 2022. Detecting Hot Spots of Methane Flux Using Footprint-Weighted Flux Maps. *Journal of Geophysical Research: Biogeosciences* 127, no. 8. doi:10.1029/2022JG006977.

Rust, F., Bodmer, P., del Giorgio, P., 2022. Modeling the spatial and temporal variability in surface water CO_2 and CH_4 concentrations in a newly created complex of boreal hydroelectric reservoirs. *Science of the Total Environment*, 815. doi:10.1016/j.scitotenv.2021.152459

Stantec Consulting Ltd., 2012. *Appendix S: Greenhouse Gases Technical Report*, in *Site C Clean Energy Project – Environmental Impact Statement, Volume 2*. Prepared for BC Hydro. Vancouver, BC. Available at: https://www.iaac-aeic.gc.ca/050/evaluations/document/93686

Teodoru, C. R., Bastien, J., Bonneville, M-C., del Giorgio, P.A., Demarty, m., Garneau, m., Hélie, J-F., Pelletier, L., Prairie, Y.T., Roulet, N.T., Strachan, I.B., and Tremblay, A., 2012. The net carbon footprint of a newly created boreal hydroelectric reservoir, *Global Biogeochem.* Cycles, 26, GB2016, doi:10.1029/2011GB004187.

Appendices

Appendix A

Tabulated Emissions

Stream	Segment	25-Apr		25-May		25-Jun		25-Jul		25-Aug		25-Sep	
		CO_2 (10^6 g C)	CH_4 (10^6 g C)	CO_2 (10^6 g C)	CH_4 (10^6 g C)	CO_2 (10^6 g C)	CH_4 (10^6 g C)	CO_2 (10^6 g C)	CH_4 (10^6 g C)	CO_2 (10^6 g C)	CH_4 (10^6 g C)	CO_2 (10^6 g C)	CH_4 (10^6 g C)
Upstream	**Segment 1 (0-5 km)**	396	0.16	766	0.36	1,238	2.99	1,068	2.25	980	2.18	1,350	1.98
	Segment 2 (5-10 km)	276	0.13	497	0.41	540	1.50	632	1.61	614	25.20	874	2.81
	Segment 3 (10-15 km)	276	0.13	496	0.41	540	1.49	632	1.61	613	25.19	874	2.81
	Segment 4 (15-20 km)	283	0.14	510	0.43	554	1.53	649	1.65	630	25.86	897	2.89
	Segment 5 (20-30 km)	1,035	0.55	1,777	1.93	1,287	4.27	2,112	6.12	2,141	148.52	3,124	13.82
	Segment 6 (30-40 km)	1,110	0.71	4,032	9.10	2,018	4.00	3,615	15.89	2,048	19.45	3,591	13.01
	Segment 7 (40-50 km)	631	0.99	2,149	4.94	956	1.24	4,409	13.92	1,614	6.36	1,596	9.54
	Segment 8 (50-60 km)	276	0.17	1,035	1.80	739	0.32	1,477	4.52	708	9.18	1,239	10.05
	Segment 9 (60-70 km)	451	0.33	1,336	7.25	526	1.44	934	8.49	1,132	14.50	1,018	9.53
	Segment 10 (70-80 km)	319	0.20	676	0.52	411	0.71	669	0.90	938	3.99	856	1.71
	Segment 11 (80-84 km)	192	0.51	177	0.10	152	0.10	190	8.03	301	0.33	206	0.27
Dam (Turbines and Spillway)	**N/A**	1,464	0.00	1,581	0.00	1,703	0.00	2,567	0.00	1,526	0.00	2,463	0.00
Downstream	**Segment 1 (0-5 km, below spillways)**	379	0.30	951	0.77	666	0.27	909	1.41	1,043	1.32	567	2.71
Total		**7,088**	**4.31**	**15,982**	**28.02**	**11,329**	**19.85**	**19,862**	**66.41**	**14,289**	**282.08**	**18,654**	**71.12**

Stream	Segment	25-Oct		25-Nov		25-Dec		26-Jan		26-Feb		26-Mar		Total	
		CO_2 (10^6 g C)	CH_4 (10^6 g C)	CO_2 (10^6 g C)	CH_4 (10^6 g C)	CO_2 (10^6 g C)	CH_4 (10^6 g C)	CO_2 (10^6 g C)	CH_4 (10^6 g C)	CO_2 (10^6 g C)	CH_4 (10^6 g C)	CO_2 (10^6 g C)	CH_4 (10^6 g C)	CO_2 (10^6 g C)	CH_4 (10^6 g C)
Upstream	**Segment 1 (0-5 km)**	1,826	5.46	1,619	4.93	864	2.63	0	0.00	0	0.00	0	0.00	**10,107**	**22.93**
	Segment 2 (5-10 km)	981	2.70	678	3.47	361	1.85	0	0.00	0	0.00	0	0.00	**5,452**	**39.68**
	Segment 3 (10-15 km)	981	2.70	677	3.47	361	1.85	0	0.00	0	0.00	0	0.00	**5,450**	**39.66**
	Segment 4 (15-20 km)	1,007	2.77	696	3.56	371	1.90	0	0.00	0	0.00	0	0.00	**5,596**	**40.73**
	Segment 5 (20-30 km)	3,011	7.60	1,511	13.06	806	6.97	0	0.00	0	0.00	0	0.00	**16,803**	**202.84**
	Segment 6 (30-40 km)	3,662	12.91	1,302	11.30	694	6.03	0	0.00	0	0.00	0	0.00	**22,072**	**92.41**
	Segment 7 (40-50 km)	1,932	18.05	696	9.88	371	5.27	0	0.00	0	0.00	0	0.00	**14,353**	**70.18**
	Segment 8 (50-60 km)	753	0.72	736	1.64	760	1.69	0	0.00	0	0.00	0	0.00	**7,723**	**30.09**
	Segment 9 (60-70 km)	1,002	2.77	508	6.28	525	6.49	526	0.27	458	0.23	390	0.20	**8,806**	**57.77**
	Segment 10 (70-80 km)	579	0.93	393	5.08	406	5.25	420	0.21	365	0.18	311	0.16	**6,344**	**19.83**
	Segment 11 (80-84 km)	212	0.27	133	1.67	267	4.44	147	0.22	128	0.19	109	0.16	**2,215**	**16.29**
Dam (Turbines and Spillway)	**N/A**	2,275	0.00	1,824	0.00	2,778	0.00	2,657	0.00	2,080	0.00	2,301	0.00	**25,220**	**0.00**
Downstream	**Segment 1 (0-5 km, below spillways)**	1,109	0.99	681	3.73	724	7.17	510	0.33	444	0.28	378	0.24	**8,361**	**19.52**
Total		**19,331**	**57.87**	**11,454**	**68.05**	**9,290**	**51.53**	**4,261**	**1.02**	**3,474**	**0.89**	**3,489**	**0.76**	**138,502**	**651.92**